Research Square

Preprints are preliminary reports that have not undergone peer review.
They should not be considered conclusive, used to inform clinical practice,
or referenced by the media as validated information.

A Computational and In Vivo Investigation into the Effects of Zeaxanthin-Lutein on the Responses of Drosophila melanogaster to Furan Toxicity

Solomon Owumi

owumisa@hotmail.com

University of Ibadan

Opeyemi A. Adeosokan
University of Ibadan

Joy Inemesit Okon
University of Ibadan

Rehoboth Ogundeji
University of Ibadan

Priscillia A. Adeseun
University of Ibadan

Abdulwasiu Ibrahim
University of Ibadan

Ibironke John Oluwasegun
University of Ibadan

Johnson K. Ehima
University of Ibadan

Emmanuel O. Ogbe
University of Ibadan

Jesutosin O. Babalola
University of Ibadan

Uche Arunsi
Georgia Institute of Technology

Moses T. Otunla
University of Kentucky

Ayomide P. Akomolafe
University of Nebraska Medical Centre

Chioma Irozuru
Montana State University

Amos O. Abolaji
University of Ibadan

Research Article

Keywords: Network-Pharmacology, furan, Drosophila melanogaster, toxicity, oxidative imbalance, lutein-zeaxanthin, and molecular docking

Posted Date: March 4th, 2026

DOI: https://doi.org/10.21203/rs.3.rs-8972251/v1

License: This work is licensed under a Creative Commons Attribution 4.0 International License. Read Full License

Additional Declarations: No competing interests reported.

Abstract

The toxic effects of environmental contaminants, such as furan, are a public health issue, prompting research into affordable, accessible treatments. *Drosophila melanogaster* is an arthropod that has been utilised as a model for human disease, as it harbours approximately 75% of human disease-related genes. Antioxidant-rich nutraceuticals may be beneficial. Lutein (L) and zeaxanthin (Z) are natural carotenoids with notable pharmacological and antioxidant effects. Network pharmacology (NP) analysis provides insight into the cellular and molecular mechanisms underlying biomolecular interactions in toxicity and chemoprevention, underscoring the importance of further *in vivo* studies. *In silico* NP exploration found 47 shared gene targets between lutein-zeaxanthin-induced protection and furan toxicity. Protein–protein interaction analysis identified ALB, APOE, IL-6, TNF, and IL-1 as central hub genes regulating gene expression and inflammation. Gene Ontology and KEGG pathway enrichment analyses revealed significant enrichment for pathways involved in cholesterol metabolism, inflammatory and immune responses, lipid transport, and protein binding. Additionally, we evaluated the protective effects of lutein-zeaxanthin (LZ) supplementation against furan-induced toxicity in *Drosophila melanogaster in vivo* by assessing oxidative imbalance in the flies' fat bodies (liver) and brains. *D. melanogaster* were exposed to Furan (100 μM) alone or supplemented with lutein-zeaxanthin combination (88μM + 18μM or 44μM + 9μM) via diet for seven consecutive days. Antioxidant enzyme activity, non-enzymatic antioxidant levels, and oxidative stress biomarkers were spectrophotometrically determined. LZ combined supplementation significantly ($p < 0.05$) restored furan-induced oxidative stress by reversing the activity of antioxidant enzymes (glutathione-*s*-transferases) and non-enzymic antioxidants (non-protein thiols) and reducing other markers of oxidative stress (total hydroperoxide) in *D. melanogaster.* Additionally, supplementation with a lutein-zeaxanthin combination increases nitric oxide and total thiol levels. Furthermore, supplementation with the lutein-zeaxanthin combination ameliorated the histopathological alterations in the fat body (liver) and brain tissues of flies caused by furan exposure. This study indicates that lutein-zeaxanthin may help prevent furan- and related chemical-induced toxicity, acting as an antioxidant-rich nutraceutical with specific pathways identified by NP as therapeutic targets. Furthermore, molecular docking simulations indicated that lutein, particularly in combination with zeaxanthin, exhibits strong binding affinity (including binding scores) to target proteins, suggesting the potential to attenuate the toxic effects of furan.

1.0 Introduction

Oxidative/nitrosative stress, the result of an imbalance between reactive oxygen/nitrogen species (RONS) and the body’s antioxidant defences, has emerged as a significant factor in the molecular pathogenesis of various chronic diseases, including cancer, neurodegenerative disorders, and other age-associated conditions, mainly through cellular and organ damage(Ibrahim & Muhammad, 2023). Recent literature has shown that diet-derived carotenoids, specifically zeaxanthin and lutein, have protective effects against RONS(Kohlstadt, 2016). These pigments, well-known for their roles in ocular health, have garnered attention for their broader implications in cellular protection, anti-inflammatory effects, and longevity (Stringham et al., 2024).

Furan (C_4H_4O) is a naturally occurring volatile (boiling point: 31°C), colourless, heterocyclic and carcinogenic organic compound (Batool et al., 2021) that is found in a variety of heat-processed foods (Arvid Fromberg, 2009) and beverages, including canned and jarred foods such as coffee, canned meats, and baby foods (Arisseto). Multiple mechanisms have been proposed for the formation of furan. These include: (i) the thermal decomposition of carbohydrates, either independently or in the presence of amino acids such as serine and cysteine; (ii) the high-temperature oxidation of ascorbic acid; and (iii) the oxidative degradation of polyunsaturated fatty acids and carotenoids. (Seok et al., 2015). Furan is known to mediate its toxicity via the functional ortholog Cyp6g1, the

Drosophila equivalent of mammalian CYP2E1, an isoform of cytochrome P450 that generates a reactive intermediate, cis-2-butene-1,4-dial (BDA) (Chung et al., 2009; Ikeno et al., 2011). This intermediate contributes to the toxicity of Furan by reacting with various biologically essential macromolecules, such as proteins and DNA, via nucleophilic reactions. Thus, the birth of chronic health conditions such as cancer and neurodegeneration via oxidative and nitrosative stress (Owumi et al., 2022). In vivo and in vitro studies have shown that furan disrupts the normal function of the epididymis, prostate gland, and testis, leading to reduced sperm production and quality, as well as reduced hormonal levels (Owumi et al., 2020; Rehman et al., 2019). Increased expression of pro-apoptotic genes, such as Caspase-3 and Caspase-9, can also be traced to furan exposure in male rats (Owumi et al., 2020). In this study, the cost-effective *Drosophila melanogaster* serves as a prominent model to investigate the protective effects of dietary antioxidants against furan-induced oxidative damage, given its established molecular, anatomical, and physiological similarities with humans (Olalekan Abolaji et al., 2014a).

As antioxidants, lutein (L) and zeaxanthin (Z) are two naturally occurring carotenoids belonging to the xanthophyll family, which are oxygenated derivatives of carotenes(Mein et al., 2011). They are structural isomers, differing only in the position of a double bond in one of the end rings (Demmig-Adams et al., 2022). Key sources of these lipophilic carotenoids include kale, savoy cabbage, spinach, broccoli, peas, parsley, corn, and egg yolks (Perry et al., 2009). Kale contains the highest amount, with about 39 mg per 100 g, followed by spinach, which provides roughly 11.9 mg per 100 g (Mrowicka et al., 2022). The recommended daily intake of lutein is approximately 10.0 mg, and that of zeaxanthin is 2 mg (Ranard et al., 2017). The defensive effects of these carotenoids are mainly related to their defence against oxidative stress and blue light damage, as well as their ability to scavenge free radicals (Abdel-Aal el et al., 2013). Lutein and zeaxanthin are the only dietary carotenoids that accumulate in the retina, specifically the macula, and are called macular pigments (Landrum & Bone, 2001). An increased level of macular pigment has been associated with a reduced risk of developing age-related macular degeneration (AMD). This inverse relationship suggests that higher concentrations of lutein and zeaxanthin in the macula may offer protective effects by filtering harmful blue light and mitigating oxidative damage to retinal cells (Mrowicka et al., 2022). The antioxidant activity of zeaxanthin and lutein is attributed to their ability to quench singlet oxygen and neutralise reactive oxygen species (ROS) (Widomska & Subczynski, 2014), thereby protecting cellular structures from oxidative stress. L/Z have been shown to exert protective effects against toxin-induced hormonal and testicular dysfunction/cell death (Owumi, Ishaya, et al., 2025), and have also been reported to enhance cognitive performance and neural function by improving insulin signalling pathways, alleviating neuroinflammation and oxidative stress, and maintaining glucose homeostasis (Kim et al., 2024).

To this end, the present study investigated the protective effect of the lutein-zeaxanthin combination against furan-induced oxidative imbalance in *D. melanogaster*. The study elucidated, for the first time, the biochemical mechanism by which diet-derived carotenoids protect the biological system against furan-induced oxidative stress and maintain organ architecture.

2.0 Materials and Methods

2.1 Stock and culture of *Drosophila melanogaster*

The Harwich strain of *D. melanogaster* was used in this study. The flies were maintained at the Fly-Hub-1, Drosophila Laboratory, Department of Biochemistry, University of Ibadan, Nigeria. The fly cultures were reared on a cornmeal-based diet containing 1% weight/volume brewer's yeast, 2% weight/volume sucrose, 1% weight/volume powdered

milk, 1% weight/volume agar, and 0.08% volume/weight nipagin, at a temperature of 25 ± 1°C with 60% relative humidity under a 12-hour light/dark cycle.

2.2 Chemicals

All chemicals used in this study were of analytical grade. Furan (99%) was purchased from Hopkin and Williams Limited, Chadwell Heath, Essex, England. Hesperidin (95%). Trunature™ Vision Complex (83.33% lutein & 16.67% zeaxanthin) was purchased from Costco.

2.3 Survival Study

A survival study was conducted to determine the optimal exposure duration and concentrations of Furan and the lutein-zeaxanthin combination. The flies' diet was mixed with Furan and lutein-zeaxanthin combination at different concentrations for each group. *D. melanogaster* of the Harwich strain of both sexes aged 1–3 days were sectioned into groups of 30 flies per replicate. This was done in 5 replicates and two independent studies.

2.3.1 Determination of Study Period and Treatment Concentration

To determine the most effective days of furan exposure for this study, the flies were housed in a vial and were dispensed into six groups (n = 30 flies) as follows: Control (2% ethanol), exposed to 10 µM, 50 µM, 100 µM, 200 µM, and 500 µM furan for 7 days. To establish the optimal days for lutein-zeaxanthin combination exposure, they were dispensed into two groups (n = 30 flies) as follows: Control (2% ethanol), exposed to 88µM + 18µM and 44µM + 9µM lutein-zeaxanthin combination for 7 days. The result of dead flies was recorded for each vial daily to calculate the percentage survival per day, and the percentage rate of survival of flies in each group was plotted against the days of exposure and the concentration of furan and lutein-zeaxanthin combination, respectively (Olalekan Abolaji et al., 2014b). Thereafter, biomarkers of toxicity, including nitric oxide (NO), total hydroperoxide, non-protein thiols (NPSH) and total thiols (TSH), were measured to determine the appropriate concentration of furan and lutein-zeaxanthin combination in this study.

2.3.2 Furan exposure and lutein-zeaxanthin combination treatment

Regarding the survival studies, wild-type *D. melanogaster* of both sexes were assigned to six groups, with 50 flies per group (n = 50). Furan and lutein-zeaxanthin combinations were carefully mixed with the flies' feed at different concentrations for individual groups. The groups are as follows: Group 1 was the control (2% ethanol), Group 2 was 100 µM concentration of Furan, Group 3 and 4 were administered 88 µM + 18 µM and 44 µM + 9 µM lutein-zeaxanthin combination, respectively, Group 5 and 6 were administered a combined concentration of 100 µM of Furan and 88 µM + 18 µM and 44 µM + 9 µM lutein-zeaxanthin combination, respectively. After a 7-day exposure period, each replicate of the groups was anaesthetised using the Ice-cold method. Subsequently, the weight of flies in each replicate group was measured and homogenised in 0.1 M phosphate buffer at pH 7.0 (1mg: 10 µL). The homogenised fly replicate was then subjected to 4000g centrifugation for 10min at 4°C. The supernatants obtained from this process were then separated from the homogenate and transferred into separately labelled microtubes for biochemical analysis, including total hydroperoxide, nitric oxide (NO), total thiols (TSH), non-protein thiols (NPSH), glutathione-s-transferase (GST)

2.5 Biochemical Examinations

2.5.1 Determination of Total Hydroperoxide Level

The total hydroperoxide level was determined according to the Wolff method (Wolff, 1994). The assay mixture was prepared by mixing 590 µL of FOX-1 reagent (Ferrous Oxidation-Xylenol orange, 10 ml of 100 mM xylenol orange, 50 ml of 250 mM ammonium ferrous sulphate, 10 mL of 100 mM sorbitol, 5 mL of 25 mM H_2SO_4 and 30 mL of distilled water) with 10 µL of the sample. A 30-minute incubation at room temperature was performed, followed by absorbance measurement at 560 nm. The concentration of the hydrogen peroxide generated was determined by extrapolating sample absorbance values from the standard curve.

2.5.2 Determination of Nitric Oxide Level

By incubating 250 µL of sample with 250 µL of Griess reagent [0.1% N-(1-naphthyl) ethylenediamine dihydrochloride; 1% sulfanilamide in 5% phosphoric acid; 1:1 ratio] at room temperature for 20 minutes, the level of nitric oxide (NO) was ascertained using the Griess reaction method. At 550 nm, the absorbance was then measured. The standard calibration curve of $NaNO_2$ was used to calculate the NO concentration in the sample (Green LC, 1982).

2.5.3 Determination of Non-protein Thiols Level

Ellman's reagent (DTNB) was used to estimate the non-protein thiol content by the colourimetric method described by Jollow et al. (Jollow DJ, 1974). The supernatant was treated with a 1:1 solution of 4% Sulphosalicylic acid after extraction. After being kept at 4°C for an hour, the samples were centrifuged for 10 minutes at 4°C at 5000 rpm. 550 µL of 0.1 M phosphate buffer, 100 µL of supernatant, and 100 µL of DTNB were included in the assay mixture. The results were expressed as moles of GSH per gram of protein, after measuring the optical density (OD) at 412 nm.

2.5.4 Determination of Total Thiols Level

The Ellman method was used to calculate the total thiol content. The reaction mixture contained 20 µL of the sample, 10 µL of DTNB, and 170 µL of 0.1 M potassium phosphate buffer (pH 7.4). After a 30-minute incubation at room temperature, absorbance was measured at 412 nm. GSH was used as the standard for each measurement, and the results were reported as µmole/mg of protein (GL, 1959).

2.5.5 Determination of Glutathione-*s*-transferase Activity

Using the technique developed by Habig and Jakoby, the activity of glutathione-S-transferase (GST; EC 2.5.1.18) was assessed. For this measurement, 1-chloro-2,4-dinitrobenzene (CDNB) served as the substrate. A solution consisting of 20 µL of 0.25 M potassium phosphate buffer, pH 7.0, with 2.5 mM EDTA, 10.5 µL of distilled water, and 500 µL of 0.1 M GSH at 25°C, 10 µL of 25 mM CDNB, and 20 µL of sample (1:5 dilution) comprised the reaction mixture, which had 270 µL. A specific volume of CDNB is also added, along with a small diluted sample. All of these ingredients were combined at 25°C. The reaction mixture was monitored at 340 nm for 5 minutes, with measurements taken every 10 seconds. Using the GST molar extinction coefficient (ε) of 9.6 $mM^{-1}cm^{-1}$, the measurements were expressed as µmol of CDNB/min/mg protein based on the data gathered (Habig & Jakoby, 1981).

2.5.6 Protein Concentration

The protein concentration in this study was determined according to the method described by Lowry (Lowry OH, 1951).

2.5.7 Histopathological Analysis of the Brain and Fat Body

Brain and fat body samples were preserved in 10% formalin for three days. After the samples were dehydrated, they were embedded in paraffin and subsequently stained with haematoxylin and eosin (H & E) stain. Pathologists, blinded to the treatment groups, evaluated and scored histopathological aberrations after viewing the tissue under a light microscope.

2.5.8 Statistical Analysis

The findings are presented as the standard error of the mean (SEM) ± the mean. Tukey's post hoc test was performed after a one-way analysis of variance (ANOVA) was used to analyse the data. Statistically significant differences were set at $p < 0.05$.

Molecular docking

After the *in vivo* studies, an *in silico* analysis, including molecular docking, was performed to investigate the interactions of furan, lutein, and zeaxanthin with GST and ACHE. Additionally, molecular docking of furan with Cytochrome P450 2E1 (CYP2E1) was performed, as CYP2E1 is the key enzyme responsible for the metabolic activation of furan into its reactive intermediate, cis-2-butene-1,4-dial. The three-dimensional structure of CYP2E1 (PDB ID: 3E6I) was retrieved from the Protein Data Bank (https://www.rcsb.org) on 16 October 2025 and cleaned using the Protein Repair and Analysis Server (http://protein-science.com/) by removing native ligands, inhibitors and crystallographic water molecules to ensure optimal docking accuracy (Nnyigide et al., 2022). Molecular structures of furan, lutein and zeaxanthin were extracted from the PubChem compound database (www.pubchem.ncbi.nlm.nih.gov) accessed on 9 September 2025) in SDF format and optimised. Open Babel was used to convert the ligand SDF files to the mol2 chemical format (O'Boyle et al., 2011). Open Babel was used for ligand optimisation, which involved minimising the ligands and converting them to PDBQT format.

The crystal structure of *D. melanogaster* GST domain in Complex with Glutathione (PDBID: 1M0U) and ACHE phosphorylated by sarin (PDBID: 5fpq) was retrieved from the Protein Data Bank (https://www.rcsb.org) on 16 September 2025. The downloaded crystal structure was cleaned using the Protein Repair & Analysis Server (http://protein-science.com/) to handle missing residues, refine side-chain orientations, and ensure structural integrity before molecular docking simulations (Nnyigide et al., 2022). Molecular docking was performed using PyRx. PyRx is a popular virtual screening technique that has been used to find several possible therapy candidates. PyRx uses AutoDock and AutoDock Vina, two score-based Lamarckian Genetic Algorithms (LGAs). AutoDock Vina was utilised to carry out autonomous docking with each of the compounds after accessing the PDB files of the target protein that was created. To explore potential binding sites on the protein, a blind docking approach was employed, maximising the search space. The search space was defined using a three-dimensional grid box with the following parameters: Centre Coordinates: X = 0.4749, Y = -9.2957, Z = 25.4424; dimensions (Å): 101.27 × 58.79 × 55.84, with a default grid spacing of 0.375Å maintained for the calculation of the grid maps.

After the compounds were eventually docked, the target protein macromolecule was visualised using the BIOVIA Discovery Studio Visualizer Software, revealing the binding interactions with specific ligands.

Using Discovery Studio software, two-dimensional (2D) interaction diagrams were generated to examine ligand-target macromolecular interactions. The protein-ligand docked first.

BIOVIA Discovery Studio Visualizer software was used to generate complexes of ligands with high binding affinities in Protein Data Bank (PDB) format. The ligand-protein interactions were then displayed in Discovery Studio after each PDB format file was opened independently.

Gene mining, target prediction and network construction

The GeneCards database (https://www.genecards.org/, accessed on September 19, 2025) was used to predict potential L/Z targets. The related targets were collected using the keywords “lutein and zeaxanthin combination

induced protection (LZP)" and the Homo sapiens species. Possible targets for furan were extracted on September 19, 2025, from CTG (Comparative Toxicogenomic Database). The goals of these datasets were combined, and target repeats were removed. Using the Bioinformatics tool Venny 2.1.0 (https://bioinfogp.cnb.csic.es/tools/venny/), accessed on September 19 2025, the mutual targets of the compounds were identified by intersecting the gene sets (Tabassum et al., 2022). Protein-protein interaction (PPI) networks were constructed using STRING (https://string-db.org/cgi/network) (Szklarczyk et al., 2023). The PPI networks were imported into Cytoscape 3.10.3 (Shannon et al., 2003). The CytoHubba plugin was used to calculate the top 10 hub nodes based on degree (k). The Analyze Network tool was used for topological analyses of the network, including the Maximal Clique Centrality (MCC) method, degree (k), betweenness centrality (BC), clustering coefficient, closeness centrality (CC), The Gene Ontology (GO) and Kyoto Encyclopedia of Genes and Genomes (KEGG) enrichment analyses of overlapping genes were further explored through using the STRING (https://string-db.org/cgi/network accessed on 20 September 2025) and Shiny GO 0.77 tool (http://bioinformatics.sdstate.edu/go/, accessed on 20 September 2025) (Ge et al., 2020), with an FDR of < 0.05 and p of < 0.05 as cut-off values, displaying the top ten results.

3.0 Result

3.1 Molecular interactions of furan, lutein and zeaxanthin with GST and ACHE

Molecular docking techniques were utilised to clarify molecular interactions between GST and the compounds furan, lutein, and zeaxanthin. The docking simulations were executed with an exhaustiveness value of 8. For each docking run, a maximum of 9 binding poses were generated. The best-docked pose was selected based on the lowest binding affinity (kcal/mol) and root-mean-square deviation (RMSD) values. The docking results revealed that furan binds to the active site of GST (PDB: 1M0U), with a binding energy of − 3.1 kcal/mol, and shows a significant intermolecular interaction with Histidine (His108), indicating a moderate binding affinity (Figs. 4A-C). Lutein exhibited a stronger interaction with the GST active site, showing a binding energy of -5.2 kcal/mol and forming a significant hydrogen bond with Glutamine at position 96 (Gln96) (Figs. 4D-F). Zeaxanthin binds to the GST active site, with a binding energy of − 3.6 kcal/mol, having a significant intermolecular interaction with Tyrosine (at Tyr54), indicating a lower binding affinity than lutein (Figs. 4G-I). Collectively, these findings suggest that lutein, with a higher binding score, may competitively displace furan from the GST active site, indicating the potential of lutein, especially in combination with zeaxanthin, as an antioxidant and ROS scavenger.

Further molecular docking simulations of acetylcholinesterase (AChE; PDB ID: 5FPQ) with furan, lutein, and zeaxanthin. Among the three, lutein showed the strongest affinity for the AChE binding pocket, with a binding energy of − 7.6 kcal·mol^{-1} and notable interactions at Leu213 and Arg90 (Fig. 5D). Zeaxanthin also demonstrated appreciable binding, with a binding energy of − 4.9 kcal·mol^{-1} (Fig. 5E). In contrast, furan exhibited the weakest interaction, with a binding energy of − 3.1 kcal·mol^{-1} (Fig. 5A-C).

In addition, molecular docking results showed that furan binds within the active site pocket of CYP2E1 with a binding energy of − 2.8 kcal/mol (Fig. 6), suggesting a relatively weak but specific interaction. The docking pose showed key hydrophobic interactions between the furan and Leu133 and Leu442, located near the heme catalytic centre. These interactions indicate that although furan exhibits limited binding affinity, its orientation toward the heme moiety supports its potential as a substrate for CYP2E1-mediated oxidation.

3.2 Targets network and protein-protein interactions

As shown in Fig. 1A, target prediction identified 88 genes associated with lutein-zeaxanthin combination-induced protection (LZP) and 3864 genes linked to furan-associated toxicity. The Venn diagram indicates that, while each compound primarily acts through distinct biochemical pathways, there is a notable overlap of 47 genes. This suggests potential molecular interaction sites where the protective actions of lutein and zeaxanthin may help mitigate furan's toxic effects. Further analysis of the protein-protein interaction network revealed the top 10 hub genes as Albumin (ALB), Apolipoprotein E (APOE), Interleukin-6 (IL6), Tumor Necrosis Factor (TNF), Interleukin-1 beta (IL1B), Hypoxia Inducible Factor 1, Alpha Subunit (HIF1A), C-reactive protein (CRP), Glutathione Peroxidase 3 (GPX3), Jun Proto-Oncogene (JUN) and Glutamate Pyruvate Transaminase (GPT) as illustrated in Fig. 1B and summarised in Table 1.

Table 1
Topological algorithms of the extracted hub genes

Hub genes	symbol	Degree	MCC	Closeness	EPC	Bottle Neck	EcCentricity	Betweenness
Albumin	ALB	32	21083928	37.67	20.3	2	0.312	250
Apolipoprotein E	APOE	27	13774920	35.16	19.7	21	0.312	135.4
Interleukin-6	IL6	26	21078840	34.66	19.3	4	0.239	89.5
Tumor Necrosis Factor	TNF	25	19774320	34.16	19.1	1	0.312	113.6
Interleukin-1 beta	IL1B	23	20473920	33.16	19.5	2	0.312	59.6
Hypoxia Inducible Factor 1, Alpha Subunit	HIF1A	22	18618013	32.66	17.8	4	0.312	190.1
C-reactive protein	CRP	22	6129600	32.25	18.2	1	0.312	63.75
Glutathione Peroxidase 3	GPX3	22	18665064	32.25	17.8	5	0.312	74
Jun Proto-Oncogene	JUN	19	18557412	30.83	17.8	2	0.312	81.9
Glutamate Pyruvate Transaminase	GPT	19	14567280	30.75	18.1	1	0.239	29.9

Topological metrics for the retrieved hub genes in the PPI network are shown in Table 1, highlighting the basic, appropriate connections that specify their functions and significance in the network.

3.3 Gene ontology and pathway enrichment of overlapping genes

Gene Ontology (GO) and pathway enrichment analysis of the identified hub genes are depicted in Fig. 2. Also, Fig. 2A shows the GO enrichment analysis, ranking the biological processes in which the hub genes identified from the PPI network are significantly involved by −log10(FDR) score, with higher scores indicating greater statistical significance. Figure 2B illustrates the GO enrichment analysis of cellular components. Figure 2C shows the

enrichment of various molecular functions among the hub genes. Figure 2D shows the pathway enrichment of the hub genes, highlighting the key signalling and metabolic pathways to which they are associated. Furthermore, Fig. 3 illustrates the cholesterol metabolic pathway from the KEGG database, with hub genes highlighted in red to indicate their positions and potential interactions within this metabolic network.

3.4 Examination of Survival Rate and Certain Biochemical Parameters

Figure 7A shows the survival rate of the flies when exposed to various concentrations of Furan, while Fig. 7B shows that of the lutein-zeaxanthin combination. The results indicated that Furan at various concentrations (10 μM, 50 μM, 100 μM, 200 μM, and 500 μM) decreased Drosophila survival rate compared with the control (2% ethanol). In contrast, no apparent decline was observed in the survival rate of flies exposed to lutein-zeaxanthin combination at 88μM + 18μM and 44μM + 9μM when compared with the control, respectively, at 7 days of exposure. Groups exposed to 10 μM and 100 μM concentrations of Furan show pronounced effects on survival, while groups exposed to 50 μM, 200 μM, and 500 μM show similar effects in the flies. In Fig. 7B, the 44μM + 9μM lutein-zeaxanthin combination had a higher survival rate than the concentration at 88μM + 18μM when compared.

3.5 Furan-Induced Toxicity in Drosophila

The effects of Furan at various concentrations on selected oxidative stress and antioxidant biomarkers in *Drosophila melanogaster* are presented in Fig. 8. There is a significant increase in total hydroperoxide levels at 10 μM, 100 μM, and 500 μM (Fig. 8AA), indicating elevated oxidative stress. Similarly, a significant increase in nitric oxide (Fig. 8B) and non-protein thiols (Fig. 8C) levels at 500μM and 100μM, respectively. In contrast, a significant increase in total thiol levels was observed across concentrations (Fig. 8D). Given the result above, the 100 μM survival concentration was adopted as the optimal exposure concentration for this study.

3.6 Effect of Lutein-zeaxanthin Combination on Selected Biomarkers

The effects of the lutein-zeaxanthin combination on selected oxidative stress and antioxidant biomarkers are shown in Fig. 9. There was no significant alteration in the level of total hydroperoxide (**9**A), nitric oxide (**B**) and total thiols (**D**) in the flies exposed to lutein-zeaxanthin combination at 88μM + 18μM and 44μM + 9μM concentration, respectively, when compared with the control group. However, a significant increase in the level of non-protein thiols (**9C**) was observed in the group exposed to a 44 μM + 9 μM concentration of the lutein-zeaxanthin combination compared with the control group.

3.7 Preventive effect of lutein-zeaxanthin combination on Furan-induced Oxidative Stress and Antioxidant Biomarkers

Figures 10 and 11 illustrate the impact of the lutein-zeaxanthin combination and furan on Drosophila after 7 days of exposure. Furan at 100μM significantly increases the level of total hydroperoxide (Fig. 10A). In contrast, the lutein-zeaxanthin combination at 44 μM + 9 μM significantly increases nitric oxide levels compared with the control (Fig. 10B). However, a non-significant alteration was observed in the nitric oxide level in the furan-exposed group. In Fig. 11, furan at a 100 μM concentration significantly increased the levels of non-protein thiols (Fig. 11A) and the activity of glutathione-*S*–transferase (Fig. 11C). In contrast, exposure to the lutein-zeaxanthin combination at 88 μM + 18 μM and 44 μM + 9 μM reverses these effects. However, Furan had no significant impact on total thiols (Fig. 11B) compared with the control.

3.8 Lutein-zeaxanthin Combination Improve Furan-induced Histological Injury

Histological characteristics of the fly's fat body and brain are presented in Figs. 12 and 13, respectively. The histology of the control and lutein-zeaxanthin combination at 44μM + 9μM shows no visible lesion in the fat body. Flies exposed to furan alone showed adipocyte atrophy and degeneration (arrows). Lutein-zeaxanthin combination at 88μM + 18μM concentration, co-exposure of furan and lutein-zeaxanthin combination at 88μM + 18μM and 44μM + 9μM showed mild atrophy of adipocytes (HE x400). The brain histology of the control and the lutein-zeaxanthin combination at 44 μM + 9 μM appeared typical. Flies exposed to furan alone showed generalised atrophy of the white matter (asterisk) and segmental neuronal loss in the grey matter (arrows). Lutein-zeaxanthin combination at 88μM + 18μM concentration shows moderate segmental atrophy of neurons in the grey matter (arrows). In contrast, co-exposure of furan and lutein-zeaxanthin combination at 88μM + 18μM and 44μM + 9μM shows atypical histological architecture similar to that of the control (HE x400).

4.0 Discussion

Drosophila melanogaster, commonly known as the fruit fly, is one of the most widely used model organisms in biological research. Its short lifespan, rapid reproduction, genetic tractability and well-mapped genome make it an ideal model for studying genetics, development, neuroscience, cancer, and toxicity (Yamaguchi & Yoshida, 2018). *Drosophila* has been an important model organism for studying the genetic foundations of diseases such as central nervous system disorders, cardiovascular disease, cancer, diabetes, and inflammatory diseases, as it has functional homologs of about 75% of the genes that cause human diseases.

Furan is a potential health risk compound that may develop in foods during cooking or heating. It is a poisonous product that has been associated with animal liver damage and cancer presence (Gruczynska, 2018). Therefore, the estimated furan intakes from the European intake definition indicate that mean dietary Furan exposures can occur in humans and infants aged 3 to 12 months at doses of 1.23 and 1.01 μg/kg bw/day, respectively (Gruczynska, 2018). Research has also shown that Furan, at a dose of 2 mg/kg body weight, can induce carcinogenic effects on rodents (Kabir & Uzzaman, 2022; Moro et al., 2012). However, the mechanism of furan-induced toxicity in *D. melanogaster* is yet to be explored.

This current study has investigated the protective effect of a lutein-zeaxanthin combination against furan-induced toxicity and multi-organ damage in *Drosophila melanogaster*. Results from this study revealed an increase in the mortality rate of exposed flies to Furan at varied concentrations (10, 50, 100, 200 and 500 μM), with a more pronounced effect at 10 and 100 μM concentrations. This can be explained by studies demonstrating the harmful effects of environmental toxins, including heavy metals and furan, on cellular composition by generating reactive species that induce oxidative stress and damage biologically essential macromolecules (such as proteins, DNA, lipids, and organs) (Alizadeh et al., 2018). Thus, the observed decline in the survival rate of flies exposed in this study indicates that Furan is detrimental and toxic to their survival and lifespan. On the contrary, previous literature has shown that supplementing flies' diet with antioxidants-nutraceuticals enhances *Drosophila's* survival rate (Nisha Sharma, 2024). However, in the current research, both lutein-zeaxanthin combinations demonstrate a moderate/negligible effect on survival.

Additionally, we assess the impact of Furan on the levels of antioxidant molecules, such as total thiol (TSH), non-protein thiols (NPSH), glutathione-*s*-transferase (GST) activity, and other markers of oxidative stress, including total

hydroperoxide and nitric oxide (NO). Zeaxanthin and lutein are carotenoids present in a wide variety of fruits and vegetables and have possible anticarcinogenic properties (M.G. Sajilata, 2008). They are well-known for their anti-inflammatory and antioxidant properties, which help prevent cancer (Ribaya-Mercado & Blumberg, 2004). The results regarding GST activity during fly exposure to furan indicate that lutein-zeaxanthin combination supplementation mitigates furan-induced activation of the antioxidant enzyme. The observed increase in the activity of the GST enzyme due to furan exposure is an indicator of an adaption response, protective response of the antioxidant defence system and cellular detoxification, which might soon cause oxidative damage and toxicity once overwhelmed (Birben et al., 2012), while both concentration of the lutein-zeaxanthin combination supplementation of flies diet significantly restored the activity of the GST enzyme. This study found that supplementing the diet with a combination of lutein and zeaxanthin enhances protective effects on the antioxidant defence system and detoxification processes in *Drosophila melanogaster*. The significant decrease in GST indicates protection against oxidative damage and enhanced cellular resilience. The result provides a more detailed description of the protective action of the lutein-zeaxanthin combination on antioxidant enzyme activity during the furan-induced adaptive response in this enzyme, thus highlighting the beneficial effect of the lutein-zeaxanthin combination as a therapeutic agent to promote health conditions linked to oxidative stress(Johra et al., 2020).

Antioxidant enzymes exert their protective role by cleansing the cell of cellular reactive oxygen and nitrogen species and free radicals. Thus, the results suggest that the lutein-zeaxanthin combination may have a protective role against the harmful effects of Furan, including inhibition of enzymatic antioxidant activity. It has been demonstrated that thiols are natural antioxidants capable of providing antioxidant defence by neutralising free radicals and reactive species, thereby ameliorating their damaging oxidant reactions(Noguchi et al., 2023). Through their sulfhydryl (SH) groups, thiols form intra- and intermolecular interactions and are complexed with reactive species. This scavenging mechanism is obtained using non-protein and total thiols during oxidative damage. This scavenging mechanism is acquired through the utilisation of non-protein and total thiols during oxidative damage. In this study, levels of non-protein thiols rise dramatically with furan exposure. Still, they are maintained at an optimum level by inclusion through feeding the flies a lutein-zeaxanthin combination into the flies' diet. This study demonstrates that non-protein thiols counteract the formation of free radicals induced by Furan and that the lutein-zeaxanthin combination can provide antioxidant action by scavenging reactive species and restoring the use of non-protein thiols. This is consistent with a study demonstrating that lutein and zeaxanthin scavenge reactive oxygen species, such as lipid peroxyl radicals and singlet oxygen (Roberts & Dennison, 2015).

Many physiological functions, including immunological responses, neurotransmission, and vasodilation, involve an intermediary nitric oxide. However, tissue damage and inflammation can be exacerbated by excess NO production, which often occurs under oxidative stress or inflammation. In the current study, dietary supplementation with the lutein-zeaxanthin combination significantly increased the observed slight furan-induced increase in NO. We hypothesised that the activity of Inducible Nitric Oxide Synthase (iNOS) may be associated with the effect of the lutein-zeaxanthin combination on NO production. Other researchers have demonstrated that lutein-zeaxanthin treatment enhances dose-dependent iNOS expression triggered by the toxicant(Abdel-Salam et al., 2017). These findings indicate that the Lutein-zeaxanthin combination specifically targets and attenuates the oxidative burden without disrupting baseline signalling (Birben et al., 2012). This demonstrates the potential therapeutic advantage of lutein-zeaxanthin in reducing inflammation-related pathology and nitrosative stress.

Total hydroperoxide refers to a group of reactive oxygen species, including hydrogen peroxide, which can trigger oxidative stress on many cellular components, including proteins, lipids and DNA. In addition, total thiols are a group of antioxidant compounds, present in both protein and non-protein molecules, that can protect cells from oxidative

stress by scavenging free radicals and other reactive species. The data from this study are consistent with previous studies showing that Furan induces oxidative stress in rodent models (Owumi et al., 2020). In our study, exposure of flies to Furan significantly increased total hydroperoxide levels, and total thiols showed a non-significant change. This oxidative stress is likely to cause the observed alterations in the histological architecture of the flies' brains and fat bodies (livers), highlighting the need for antioxidative therapy to control oxidative damage and re-establish redox homeostasis. However, supplementing the diet with a lutein-zeaxanthin combination also markedly reconstitutes brain histological architecture to normal, but with some percentage in the fat body (liver).

A molecular docking simulation showing the interaction between furan, lutein, zeaxanthin, and Glutathione-S-transferase (GST) supports our findings from *in vivo* studies that *Drosophila melanogaster* can increase the expression of oxidative-stress response markers as one of its mechanisms of adaptive response. Persistent exposure to toxicants like furan can lead to gene duplication and overexpression of GST genes (Dong et al., 2016). This adaptive mechanism is key to survival upon exposure to toxicants, as GST expression can help maintain a proper GSH/GSSG balance, which is critical for redox signalling and cellular survival under stress.

Lutein and Zeaxanthin (L/Z) synergistically enhance the Glutathione system (GSH) and increase GST activity when exposed to oxidative stress. Various mechanisms of L/Z's antioxidative and protective role include the activation of nuclear factor erythroid 2-related factor 2 (Nrf2) (Frede et al., 2017). Activation of Nrf2 stimulates the expression of endogenous antioxidants, such as GST. It may help scavenge reactive oxygen species, serving as a unique adaptive and tolerance response to toxin-induced oxidative stress (Owumi, Chimezie, et al., 2025).

Comparing increases in expression of the GstD1 and GstE1 genes, which encode GST, in response to L/Z and furan could help us understand the complex mechanisms underlying *Drosophila melanogaster's* tolerance to toxicants and its cellular adjustments to antioxidants. Temporary spikes in GST levels on furan exposure as a result of adaptive response to toxicant may lead to a measurable increase in death rate, as observed in the survival studies. Experimental studies on comprehensive datasets from molecular docking simulations emphasise the ability of lutein, with a docking score of about − 5.2 kcal/mol, to competitively bind and displace furan (docking score of -3.1 kcal/mol) at the ninaD receptor in the midgut of *Drosophila melanogaster*. (Voolstra et al., 2006).

The findings from molecular interactions on GSH with furan, lutein and zeaxanthin are consistent with further molecular docking interactions on Acetylcholinesterase (ACHE) with furan, lutein and zeaxanthin. Disrupted neuronal and motor functions resulting from elevated furan levels, which may lead to reduced exploratory activity and poor climbing performance in *Drosophila melanogaster*, could be mitigated by the combined effects of lutein and zeaxanthin (Mrowicka et al., 2022). Although L/Z can minimise the deleterious effects of chemically induced toxicity, their precise function within the broader "adaptive response" in insects is less clear than their well-established roles in mammals. Further studies should be conducted to elucidate a broader adaptive response involving L/Z in transgenic *Drosophila melanogaster*.

The application of Network pharmacology in this study provides a better understanding of the role of the lutein-zeaxanthin combination in the adaptive response to furan. The network analysis revealed 47 hub genes that may be associated with the lutein-zeaxanthin combination's preventive action against furan-induced toxicity. Ten hub genes (ALB, APOE, IL6, TNF, IL1B, HIF1A, CRP, GPX3, JUN, and GPT) were identified by analysing the protein-protein interactions of these genes. They were discovered to have the most involvement in the network. These genes participate in various life processes, including biological processes, cellular and metabolic functions, and in oxidative stress responses. The ALB and GPX3 genes are involved in the oxidative stress response and antioxidant defence. GPX3 is an extracellular (plasma) glutathione peroxidase that scavenges hydrogen peroxide and other

reactive oxygen species, thus protecting tissues from oxidative damage(Shi et al., 2022). It has been reported that reduced GPX3 expression leads to upregulation of NOX4 and enhanced oxidative stress in kidney disease models. Also, GPX3 knockdown has been reported to increase mitochondrial dysfunction and oxidative stress, linking it to tissue senescence (Song et al., 2024; Zhang et al., 2024). ALB exerts antioxidant effects in plasma by binding free radicals and transition metals, acting as a buffer against oxidative stress via its thiol groups. Low albumin levels correlate with increased oxidative stress markers in patients with malnutrition and liver disease (Arques, 2018). (JUN and HIF1A) are signal transduction and transcription factors. JUN is a core component of the AP-1 transcription factor complex, which integrates extracellular signals growth factors, stress, cytokines) into transcriptional responses (Meng & Xia, 2011). HIF1A plays a role in cellular redox status, signalling, and can modulate inflammatory genes. HIF-1α may induce inflammation by downregulating PPARG (Ajoolabady et al., 2024). (APOE, IL6, TNF, IL1B and CRP) They are involved in inflammation and inflammatory signalling in humans. They play key roles in inflammation, immune responses, and acute-phase signalling (Cacabelos et al., 2018; Zhao et al., 2023). (GPT and APOE) They are involved in various metabolic processes, including lipid metabolism and energy metabolism. The high network connectivity of genes such as IL6, TNF, IL1B, and CRP suggests their central role in furan-induced oxidative stress and inflammatory responses, and the potential of lutein-zeaxanthin to reverse and mediate these responses. ALB and GPX3 are crucial in redox balance, cell survival, and recovery from oxidative stress, supporting the idea that lutein-zeaxanthin enhances these protective mechanisms. The Topological algorithms' results for the hub genes indicate that ALB and APOE consistently have higher values across all the metrics analysed (Degree, MCC, Closeness, EPC, Bottleneck, EcCentricity, and Betweenness), highlighting their significance within the PPI network in relation to lutein-zeaxanthin combination-induced protection and furan-induced toxicity.

The ALB and APOE genes have the highest degrees, showing that they are the most influential and strongly connected nodes. ALB and IL6 genes have the highest MCC values. Maximal Clique Centrality (MCC) is a metric that identifies the most critical and central nodes within multiple cliques. The high MCC values for ALB and IL6 suggest their participation in critical, cohesive functional modules. Closeness centrality is defined as the reciprocal of the average shortest-path distance from a node to all other nodes in the network. ALB and APOE have the highest closeness values, indicating that the signal propagates faster from one node to others and that these genes can swiftly affect other nodes, highlighting their possible role in rapid cellular responses. A node's influence is measured by the Edge Percolation Centrality (EPC) analysis, which accounts for biological signals or information percolating down its edges. ALB and APOE have the highest EPC values, suggesting that they are highly involved in mediating biological processes through the network. Betweenness is one of the most important topological properties of a network. It measures the number of shortest paths that pass through a specific node; hence, it is similar to the bottleneck. Nodes with the highest betweenness and bottleneck values control most of the network's information flow, representing its critical points. The ALB and APOE genes have the highest betweenness and bottleneck values, indicating that they play essential roles in maintaining network integrity.

The enrichment analysis of the hub genes suggests pivotal roles in various biological processes, including lipid metabolism and transport, glutathione metabolism, cellular detoxification, and cellular oxidant detoxification. Top hub genes such as ALB and APOE are involved in lipid metabolism, particularly cholesterol and triglyceride transport. Furan exposure can increase blood lipid levels, including cholesterol, triglycerides, and LDL (low-density lipoprotein) cholesterol (Zhao et al., 2023), implicating genes such as ALB and APOE and strengthening our hypothesis that a Lutein-zeaxanthin combination may improve lipoprotein profiles and reduce inflammation. Moreover, APOE protects neurons indirectly by stabilising membranes and reducing lipid peroxidation. The identification of IL6, TNF, IL1B, and CRP as hub genes in the present network pharmacology analysis highlights their

central role in mediating the interplay between oxidative stress and inflammation. These genes represent critical nodes in the ROS–cytokine axis, where excessive generation of reactive oxygen species (ROS) triggers inflammatory cascades, further amplifying oxidative damage. The identification of IL6, TNF, IL1B, and CRP as hub genes in the present network pharmacology analysis highlights their central role in mediating the interplay between oxidative stress and inflammation. Although *Drosophila melanogaster* lacks canonical mammalian cytokines like IL-6 and TNF-α, it possesses highly conserved functional orthologs that drive analogous inflammatory and immune responses (Lemaitre & Hoffmann, 2007).

Specifically, the mammalian TNF signalling axis is represented in *Drosophila* by the ligand Eiger (egr) and its receptor Wengen (wgn), which are primary mediators of JNK-dependent apoptosis and stress responses following xenobiotic insult (Igaki et al., 2002). Similarly, while a direct structural ortholog for IL-6 is absent, the fly utilises the Unpaired (upd1, upd2, upd3) ligands. These ligands activate the JAK/STAT pathway, performing the same roles as IL-6 in regulating systemic energy metabolism, growth, and the 'acute phase' response to chemical (Jiang et al., 2009). Furthermore, the vertebrate IL-1β signalling pathway is functionally mirrored by the *Drosophila* Toll and IMD pathways, where the activation of NF-κB-like transcription factors (Dorsal and Relish) governs the production of antimicrobial peptides and pro-inflammatory mediators (Ganesan et al., 2011). The inclusion of CRP as a hub gene further underscores the systemic nature of the inflammatory insult; in flies, this is reflected by the upregulation of opsonin-like molecules and thioester-containing proteins (TEPs), which serve as primitive acute-phase reactants. By relating these human hub genes to their fly orthologs (egr, upd, and Relish), our network pharmacology findings provide a robust translational framework, suggesting that furan-induced oxidative stress in *Drosophila* operates through conserved pathways highly relevant to human inflammatory pathology. Finally, network pharmacology typically relies on databases derived from human clinical data, which may not capture the unique tissue-specific expression patterns found in the fly, such as those in the specialised fat body or Malpighian tubules. Lutein and zeaxanthin may counteract the pathological effects mediated by these hub genes through both antioxidant and anti-inflammatory mechanisms. As potent scavengers of ROS, these carotenoids directly mitigate oxidative burden and prevent lipid peroxidation. By lowering ROS levels, lutein and zeaxanthin can suppress NF-κB activation and inflammasome signalling, thereby reducing the expression of IL6, TNF, and IL1B.

In this way, lutein and zeaxanthin not only restore redox balance but also attenuate downstream inflammatory responses, disrupting the vicious cycle of oxidative stress and inflammation.

5.0 Conclusion

In conclusion, this study indicates that lutein-zeaxanthin combination supplementation remarkably restored the biochemical alterations induced by Furan in *Drosophila melanogaster*. A key piece of evidence supporting these findings is that the lutein-zeaxanthin combination demonstrates a protective effect against furan-induced oxidative stress by inhibiting total hydroperoxide formation, preserving non-protein thiol and total thiol levels, and restoring antioxidant enzyme activity (GST), as depicted in our proposed mechanism of protection (Fig. 14**)**. Thus, the study indicated that oxidative stress and organ damage (brain and fat body) are involved in furan toxicity. In addition, the combination of zeaxanthin and lutein prevents furan toxicity by ameliorating oxidative stress and restoring tissue architecture. Therefore, further study is required to elucidate the molecular mechanism of action by which the lutein-zeaxanthin combination restores furan-induced oxidative stress and tissue damage. This will provide novel insights into the molecular mechanisms by which antioxidants protect against environmental toxicity.

Declarations

Disclosure statement

No potential conflict of interest was reported by the author(s).

Funding

The authors privately funded this research through their contributions and received no external grants from funding agencies in the commercial, not-for-profit, or public sectors.

Author Contribution

All authors participated in the design, interpretation, and analysis of the study's data. SO, AOA, JOB conceptualised the study; SO, OAA, JIO, RO, PAA, AI, IJO, JKE, EOO, JOB, UA, MTO, APA, CI, NHS, and AOA conducted the research and analysed the preliminary data. SO, AOA, AI, IJO, JKE, EOO, and AOA supervised the investigation. SO, AI, IJO, JOB, JKE, EOO, UA, MTO, APA, CI, NHS, and AOA Proof checked the data for errors. IJO, JKE, EEO, JOB, UA, NHS, and SO conducted the *in silico* study. SO, OAA, JIO, RO, PAA, AI, IJO, JKE, EOO, JOB, UA, MTO, APA, CI, NHS, and AOA wrote and revised the manuscript.

Data Availability

The datasets used and analysed during the current study are available from the corresponding author upon reasonable request.

References

1. Abdel-Aal el SM, Akhtar H, Zaheer K, Ali R (2013) Dietary sources of lutein and zeaxanthin carotenoids and their role in eye health. Nutrients 5(4):1169–1185. https://doi.org/10.3390/nu5041169
2. Abdel-Salam OME, Youness ER, Mohammed NA, Yassen NN, Khadrawy YA, El-Toukhy SE, Sleem AA (2017) Nitric oxide synthase inhibitors protect against brain and liver damage caused by acute malathion intoxication. Asian Pac J Trop Med 10(8):773–786. https://doi.org/10.1016/j.apjtm.2017.07.018
3. Ajoolabady A, Pratico D, Lin L, Mantzoros CS, Bahijri S, Tuomilehto J, Ren J (2024) Inflammation in atherosclerosis: pathophysiology and mechanisms. Cell Death Dis 15(11):817. https://doi.org/10.1038/s41419-024-07166-8
4. Alizadeh M, Barati M, Saleh-Ghadimi S, Roshanravan N, Zeinalian R, Jabbari M (2018) Industrial furan and its biological effects on the body systems. J Food Biochem 42(5). https://doi.org/10.1111/jfbc.12597
5. Arisseto AP Food Hygiene and Toxicology in Ready-to-Eat Foods. https://doi.org/https://doi.org/https://doi.org/10.1016/B978-0-12-801916-0.00021-2
6. Arques S (2018) Human serum albumin in cardiovascular diseases. Eur J Intern Med 52:8–12. https://doi.org/10.1016/j.ejim.2018.04.014
7. Arvid Fromberg SF, Granby K (2009) Furan in heat processed food products including home cooked food products and ready-to-eat products. EFSA Supporting
8. Volum *6*(Issue 9). https://doi.org/0.2903/sp.efsa.2009.EN-1

9. Batool Z, Xu D, Zhang X, Li X, Li Y, Chen Z, Li B, Li L (2021) A review on furan: Formation, analysis, occurrence, carcinogenicity, genotoxicity and reduction methods. Crit Rev Food Sci Nutr 61(3):395–406. https://doi.org/10.1080/10408398.2020.1734532
10. Birben E, Sahiner UM, Sackesen C, Erzurum S, Kalayci O (2012) Oxidative stress and antioxidant defense. World Allergy Organ J 5(1):9–19. https://doi.org/10.1097/WOX.0b013e3182439613
11. Cacabelos R, Meyyazhagan A, Carril JC, Cacabelos P, Teijido O (2018) Pharmacogenetics of Vascular Risk Factors in Alzheimer's Disease. J Pers Med 8(1). https://doi.org/10.3390/jpm8010003
12. Chung H, Sztal T, Pasricha S, Sridhar M, Batterham P, Daborn PJ (2009) Characterisation of Drosophila melanogaster cytochrome P450 genes. Proc Natl Acad Sci U S A 106(14):5731–5736. https://doi.org/10.1073/pnas.0812141106
13. Demmig-Adams B, Polutchko SK, Adams WW (2022) Structure-Function-Environment Relationship of the Isomers Zeaxanthin and Lutein. Photochem 2(2):308–325
14. Dong H, Gill S, Curran IH, Williams A, Kuo B, Wade MG, Yauk CL (2016) Toxicogenomic assessment of liver responses following subchronic exposure to furan in Fischer F344 rats. Arch Toxicol 90(6):1351–1367. https://doi.org/10.1007/s00204-015-1561-2
15. Frede K, Ebert F, Kipp AP, Schwerdtle T, Baldermann S (2017) Lutein Activates the Transcription Factor Nrf2 in Human Retinal Pigment Epithelial Cells. J Agric Food Chem 65(29):5944–5952. https://doi.org/10.1021/acs.jafc.7b01929
16. Ganesan S, Aggarwal K, Paquette N, Silverman N (2011) NF-kappaB/Rel proteins and the humoral immune responses of Drosophila melanogaster. Curr Top Microbiol Immunol 349:25–60. https://doi.org/10.1007/82_2010_107
17. Ge SX, Jung D, Yao R (2020) ShinyGO: a graphical gene-set enrichment tool for animals and plants. Bioinformatics 36(8):2628–2629. https://doi.org/10.1093/bioinformatics/btz931
18. GL E (1959) Tissue Sulfhydryl Groups 82(70):7
19. Green LC, Glogowski WD, Skipper J, Wishnok PL, Tannenbaum JS SR (1982) Analysis of nitrate, nitrite, and [15 N]nitrate in biological fluids. Anal Biochem 126(131):8
20. Gruczynska E, Kowalska D, Kozlowska M, Majewska E, Tarnowska K (2018) Furan in roasted, ground and brewed coffee. Rocz Panstw Zakl Hig
21. Habig WH, Jakoby WB (1981) Assays for differentiation of glutathione S-transferases. Methods Enzymol 77:398–405. https://doi.org/10.1016/s0076-6879(81)77053-8
22. Ibrahim A, Muhammad SA (2023) Antioxidant-Rich Nutraceutical as a Therapeutic Strategy for Sickle Cell Disease. J Am Nutr Assoc 42(6):588–597. https://doi.org/10.1080/27697061.2022.2108930
23. Igaki T, Kanda H, Yamamoto-Goto Y, Kanuka H, Kuranaga E, Aigaki T, Miura M (2002) Eiger, a TNF superfamily ligand that triggers the Drosophila JNK pathway. EMBO J 21(12):3009–3018. https://doi.org/10.1093/emboj/cdf306
24. Ikeno T, Katagiri C, Numata H, Goto SG (2011) Causal involvement of mammalian-type cryptochrome in the circadian cuticle deposition rhythm in the bean bug Riptortus pedestris. Insect Mol Biol 20(3):409–415. https://doi.org/10.1111/j.1365-2583.2011.01075.x
25. Jiang H, Patel PH, Kohlmaier A, Grenley MO, McEwen DG, Edgar BA (2009) Cytokine/Jak/Stat signalling mediates regeneration and homeostasis in the Drosophila midgut. Cell 137(7):1343–1355. https://doi.org/10.1016/j.cell.2009.05.014

26. Johra FT, Bepari AK, Bristy AT, Reza HM (2020) A Mechanistic Review of beta-Carotene, Lutein, and Zeaxanthin in Eye Health and Disease. Antioxid (Basel) 9(11). https://doi.org/10.3390/antiox9111046
27. Jollow DJ, Jampaglione MJ, Gillette N JR (1974) Bromobenzene-induced liver necrosis. Protective role of glutathione and evidence for 3,4-bromobenzene oxide as the hepatotoxic metabolite. Pharmacology 11(151):69
28. Kabir E, Uzzaman M (2022) A review on biological and medicinal impact of heterocyclic compounds. Results Chem 4. https://doi.org/10.1016/j.rechem.2022.100606
29. Kim DS, Kang S, Moon NR, Shin BK, Park S (2024) Zeaxanthin and Lutein Ameliorate Alzheimer's Disease-like Pathology: Modulation of Insulin Resistance, Neuroinflammation, and Acetylcholinesterase Activity in an Amyloid-beta Rat Model. Int J Mol Sci 25(18). https://doi.org/10.3390/ijms25189828
30. Kohlstadt I (2016) *Food and Nutrients in Disease Management* (1st edition ed.). CRC press. https://doi.org/https://doi.org/10.1201/9781420067637
31. Landrum JT, Bone RA (2001) Lutein, zeaxanthin, and the macular pigment. Arch Biochem Biophys 385(1):28–40. https://doi.org/10.1006/abbi.2000.2171
32. Lemaitre B, Hoffmann J (2007) The host defense of Drosophila melanogaster. Annu Rev Immunol 25:697–743. https://doi.org/10.1146/annurev.immunol.25.022106.141615
33. Lowry OH, Farr RN, Randall AL RJ (1951) Protein measurement with the Folin phenol reagent. J Biol Chem 193(265):75. https://www.ncbi.nlm.nih.gov/pubmed/14907713
34. Sajilata MG, Kamat RSSMY (2008) The Carotenoid Pigment Zeaxanthin—A Review. *Comprehensive Reviews in Food Science and Food Safety*
35. Volume *7*(Issue 1), pp. 29–49. https://doi.org/https://doi.org/10.1111/j.1541-4337.2007.00028.x
36. Mein JR, Dolnikowski GG, Ernst H, Russell RM, Wang XD (2011) Enzymatic formation of apo-carotenoids from the xanthophyll carotenoids lutein, zeaxanthin and beta-cryptoxanthin by ferret carotene-9',10'-monooxygenase. Arch Biochem Biophys 506(1):109–121. https://doi.org/10.1016/j.abb.2010.11.005
37. Meng Q, Xia Y (2011) c-Jun, at the crossroad of the signaling network. Protein Cell 2(11):889–898. https://doi.org/10.1007/s13238-011-1113-3
38. Moro S, Chipman JK, Wegener JW, Hamberger C, Dekant W, Mally A (2012) Furan in heat-treated foods: formation, exposure, toxicity, and aspects of risk assessment. Mol Nutr Food Res 56(8):1197–1211. https://doi.org/10.1002/mnfr.201200093
39. Mrowicka M, Mrowicki J, Kucharska E, Majsterek I (2022) Lutein and Zeaxanthin and Their Roles in Age-Related Macular Degeneration-Neurodegenerative Disease. Nutrients 14(4). https://doi.org/10.3390/nu14040827
40. Nisha Sharma DS, Rajesh K, Kesharwani RK, Keservani P, Gupta C (2024) Advances in Flavonoids for Human Health and Prevention of Diseases [Book]. *Apple Academic Press, Incorporated*, *Edition 1*, 304
41. Nnyigide OS, Nnyigide TO, Lee SG, Hyun K (2022) Protein Repair and Analysis Server: A Web Server to Repair PDB Structures, Add Missing Heavy Atoms and Hydrogen Atoms, and Assign Secondary Structures by Amide Interactions. J Chem Inf Model 62(17):4232–4246. https://doi.org/10.1021/acs.jcim.2c00571
42. Noguchi N, Saito Y, Niki E (2023) Actions of Thiols, Persulfides, and Polysulfides as Free Radical Scavenging Antioxidants. Antioxid Redox Signal 39(10–12):728–743. https://doi.org/10.1089/ars.2022.0191
43. O'Boyle NM, Banck M, James CA, Morley C, Vandermeersch T, Hutchison GR (2011) Open Babel: An open chemical toolbox. J Cheminform 3:33. https://doi.org/10.1186/1758-2946-3-33
44. Olalekan Abolaji A, Paul Kamdem J, Henrique Lugokenski T, Nascimento K, Pansera Waczuk T, Farombi EO, da Silva Loreto E, E. L., Rocha T, J. B (2014a) Involvement of oxidative stress in 4-vinylcyclohexene-induced toxicity

in Drosophila melanogaster. Free Radic Biol Med 71:99–108. https://doi.org/10.1016/j.freeradbiomed.2014.03.014

45. Olalekan Abolaji A, Paul Kamdem J, Henrique Lugokenski T, Nascimento K, Pansera Waczuk T, Farombi EO, da Silva Loreto E, E. L., Rocha T, J. B (2014b) Involvement of oxidative stress in 4-vinylcyclohexene-induced toxicity in Drosophila melanogaster. Free Radic Biol Med 71:99–108. https://doi.org/10.1016/j.freeradbiomed.2014.03.014
46. Owumi S, Chimezie J, Salami MO, Ishaya JA, Onyemuwa CV, Nnamdi M, Owoeye O (2025) Lutein and Zeaxanthin abated neurobehavioral, neurochemical and oxido-inflammatory derangement in rats intoxicated with Aflatoxin B(1). Toxicon 258:108345. https://doi.org/10.1016/j.toxicon.2025.108345
47. Owumi S, Ishaya JA, Chimezie J, Nnamdi M, Chibuzor J, Joel FO, Babalola JO (2025) Aflatoxin B(1)-induced toxicity, oxido-inflammatory damage, and apoptosis in male rat reproductive circuitry were abrogated by co-treating with the xanthophyll-lutein and zeaxanthin. Mycotoxin Res 41(3):513–527. https://doi.org/10.1007/s12550-025-00600-6
48. Owumi SE, Adedara IA, Farombi EO, Oyelere AK (2020) Protocatechuic acid modulates reproductive dysfunction linked to furan exposure in rats. Toxicology 442:152556. https://doi.org/10.1016/j.tox.2020.152556
49. Owumi SE, Arunsi UO, Otunla MT, Oluwasuji IO (2022) Exposure to lead and dietary furan intake aggravates hypothalamus-pituitary-testicular axis toxicity in chronic experimental rats. J Biomed Res 37(2):100–114. https://doi.org/10.7555/JBR.36.20220108
50. Perry A, Rasmussen H, Johnson EJ (2009) Xanthophyll (lutein, zeaxanthin) content in fruits, vegetables and corn and egg products. J Food Compos Anal 22(1):9–15. https://doi.org/https://doi.org/10.1016/j.jfca.2008.07.006
51. Ranard KM, Jeon S, Mohn ES, Griffiths JC, Johnson EJ, Erdman JW Jr. (2017) Dietary guidance for lutein: consideration for intake recommendations is scientifically supported. Eur J Nutr 56(Suppl 3):37–42. https://doi.org/10.1007/s00394-017-1580-2
52. Rehman H, Jahan S, Ullah I, Winberg S (2019) Toxicological effects of furan on the reproductive system of male rats: An in vitro and in vivo-based endocrinological and spermatogonial study. Chemosphere 230:327–336. https://doi.org/10.1016/j.chemosphere.2019.05.063
53. Ribaya-Mercado JD, Blumberg JB (2004) Lutein and zeaxanthin and their potential roles in disease prevention. J Am Coll Nutr 23(6 Suppl):567S–587S. https://doi.org/10.1080/07315724.2004.10719427
54. Roberts JE, Dennison J (2015) The Photobiology of Lutein and Zeaxanthin in the Eye. *J Ophthalmol*, *2015*, 687173. https://doi.org/10.1155/2015/687173
55. Seok YJ, Her JY, Kim YG, Kim MY, Jeong SY, Kim MK, Lee JY, Kim CI, Yoon HJ, Lee KG (2015) [Not Available]. Toxicol Res 31(3):241–253. https://doi.org/10.5487/TR.2015.31.3.241(Furan in Thermally Processed Foods - A Review.)
56. Shannon P, Markiel A, Ozier O, Baliga NS, Wang JT, Ramage D, Amin N, Schwikowski B, Ideker T (2003) Cytoscape: a software environment for integrated models of biomolecular interaction networks. Genome Res 13(11):2498–2504. https://doi.org/10.1101/gr.1239303
57. Shi L, Chen B, Wang X, Huang M, Qiao C, Wang J, Wang Z (2022) Antioxidant response to severe hypoxia in Brandt's vole Lasiopodomys brandtii. Integr Zool 17(4):581–595. https://doi.org/10.1111/1749-4877.12602
58. Song Y, Zhu M, Islam MA, Gu W, Alim K, Cheng CS, Chen J, Xu Y, Xu H (2024) Glutathione peroxidase 3 is essential for countering senescence in adipose remodelling by maintaining mitochondrial homeostasis. Redox Biol 77:103365. https://doi.org/10.1016/j.redox.2024.103365

59. Stringham NT, Green M, Roche W, Prado-Cabrero A, Mulcahy R, Nolan J (2024) Lutein, zeaxanthin, and meso-zeaxanthin supplementation attenuates inflammatory cytokines and markers of oxidative cardiovascular processes in humans. Nutr Metab Cardiovasc Dis 34(8):1976–1983. https://doi.org/10.1016/j.numecd.2024.05.009
60. Szklarczyk D, Kirsch R, Koutrouli M, Nastou K, Mehryary F, Hachilif R, Gable AL, Fang T, Doncheva NT, Pyysalo S, Bork P, Jensen LJ, von Mering C (2023) The STRING database in 2023: protein-protein association networks and functional enrichment analyses for any sequenced genome of interest. Nucleic Acids Res 51(D1):D638–D646. https://doi.org/10.1093/nar/gkac1000
61. Tabassum S, Khalid HR, Haq Wu, Aslam S, Alshammari A, Alharbi M, Riaz Rajoka MS, Khurshid M, Ashfaq UA (2022) Implementation of System Pharmacology and Molecular Docking Approaches to Explore Active Compounds and Mechanism of Ocimum Sanctum against Tuberculosis. Processes 10(2). https://doi.org/10.3390/pr10020298
62. Voolstra O, Kiefer C, Hoehne M, Welsch R, Vogt K, von Lintig J (2006) The Drosophila class B scavenger receptor NinaD-I is a cell surface receptor mediating carotenoid transport for visual chromophore synthesis. Biochemistry 45(45):13429–13437. https://doi.org/10.1021/bi060701u
63. Widomska J, Subczynski WK (2014) Why has Nature Chosen Lutein and Zeaxanthin to Protect the Retina? J Clin Exp Ophthalmol 5(1):326. https://doi.org/10.4172/2155-9570.1000326
64. Wolff SP (1994) [18] Ferrous ion oxidation in presence of ferric ion indicator xylenol orange for measurement of hydroperoxides. In *Methods in enzymology* (Vol. 233, pp. 182–189). Academic Press. https://doi.org/https://doi.org/10.1016/S0076-6879(94)33021-2
65. Yamaguchi M, Yoshida H (2018) Drosophila as a Model Organism. Adv Exp Med Biol 1076:1–10. https://doi.org/10.1007/978-981-13-0529-0_1
66. Zhang N, Liao H, Lin Z, Tang Q (2024) Insights into the Role of Glutathione Peroxidase 3 in Non-Neoplastic Diseases. Biomolecules 14(6). https://doi.org/10.3390/biom14060689
67. Zhao X, Niu Y, Zhao XL, Ruan HJ, Xiang Y, Wang LY, Feng Y, Tang QY (2023) Associations Between Serum TNF-alpha, IL-6, hs-CRP and GLMD in Obese Children and Adolescents: A Cross-Sectional Study. Diabetes Metab Syndr Obes 16:3915–3923. https://doi.org/10.2147/DMSO.S434482
68. Legend to Figures

Figures

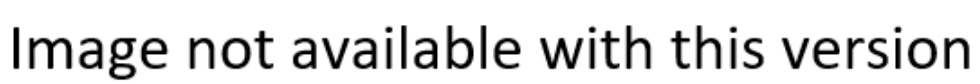


Figure 1

(**A**) Venn diagram showing the intersection between genes targeted by furan and L/Z induced protection (LZP). (**B**) Protein-protein interaction (PPI) network of the 47 common genes between furan and LZP. The network shows interactions among proteins encoded by these genes.

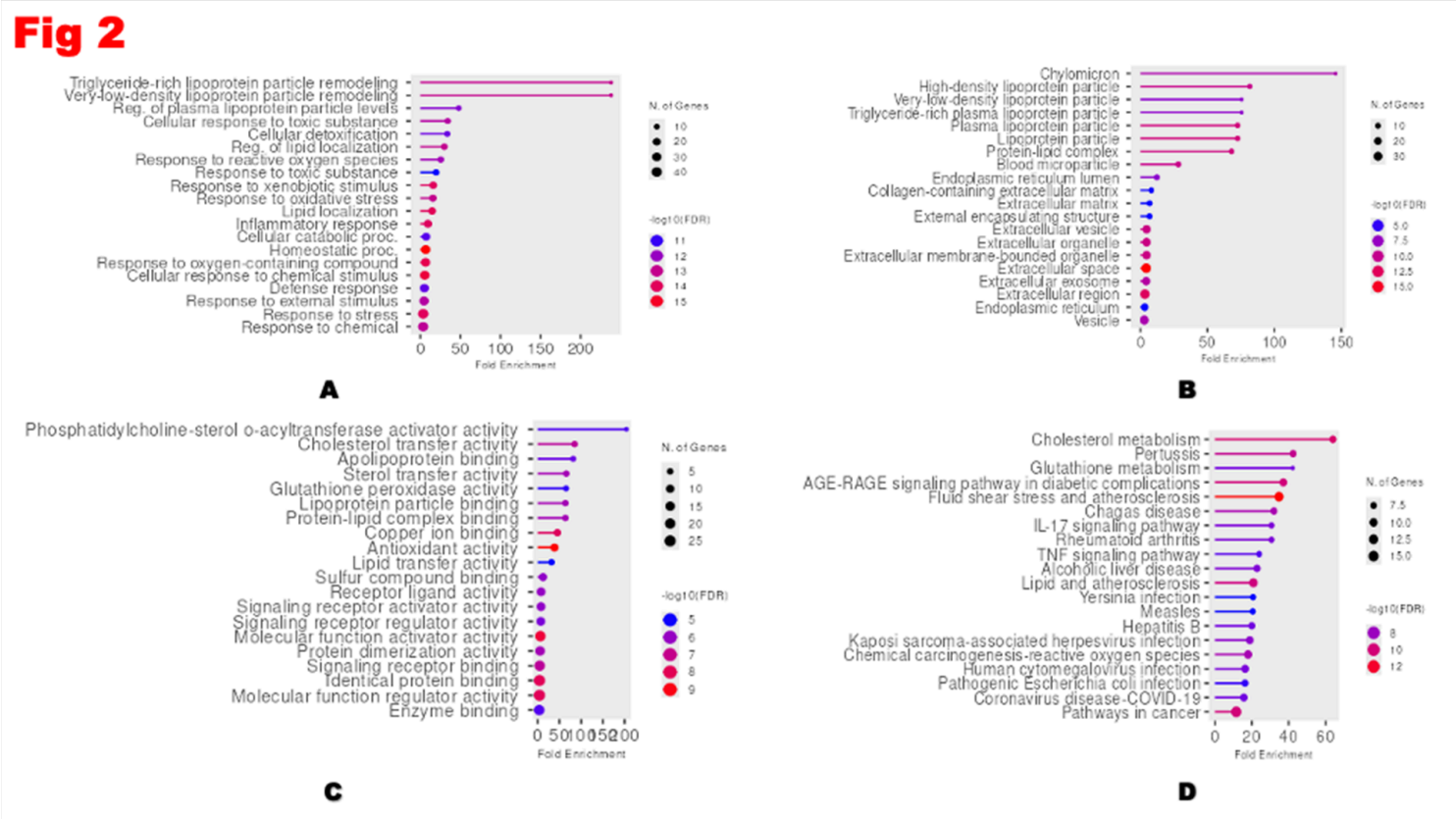


Figure 2

Gene ontology of common genes related to furan and L/Z induced protection (LZP). (**A**) Biological Process Enrichment: The graph shows the most significantly enriched biological processes related to the hub genes, ranked by fold enrichment. Top processes include Triglyceride-rich lipoprotein particle remodelling, Very-low-density lipoprotein particle remodelling, and High-density lipoprotein particle remodelling. The colour gradient indicates the -log10 of the false discovery rate (FDR), with higher values indicating more vital significance. (**B**) Cellular Component Enrichment: The most enriched cellular components are shown in this graph, illustrating critical structures such as the immediate-density lipoprotein particle, the chylomicron interleukin-6 receptor complex, the chromatin lock complex, and very-low-density lipoprotein particles. (**C**) Molecular Function Enrichment: The graph displays the top enriched molecular functions, including phosphatidylcholine-sterol O-acyltransferase activator activity, lipoprotein lipase activity, complement component C1q complex binding, and cholesterol transfer activity. (**D**) KEGG Pathway Enrichment: The graph shows the top enriched KEGG pathways, including cholesterol metabolism, Pertussis, glutathione metabolism. The size of the dots corresponds to the number of genes involved in each pathway, while the colour gradient reflects -log10(FDR), with red dots indicating the most significant pathways.

Fig 3

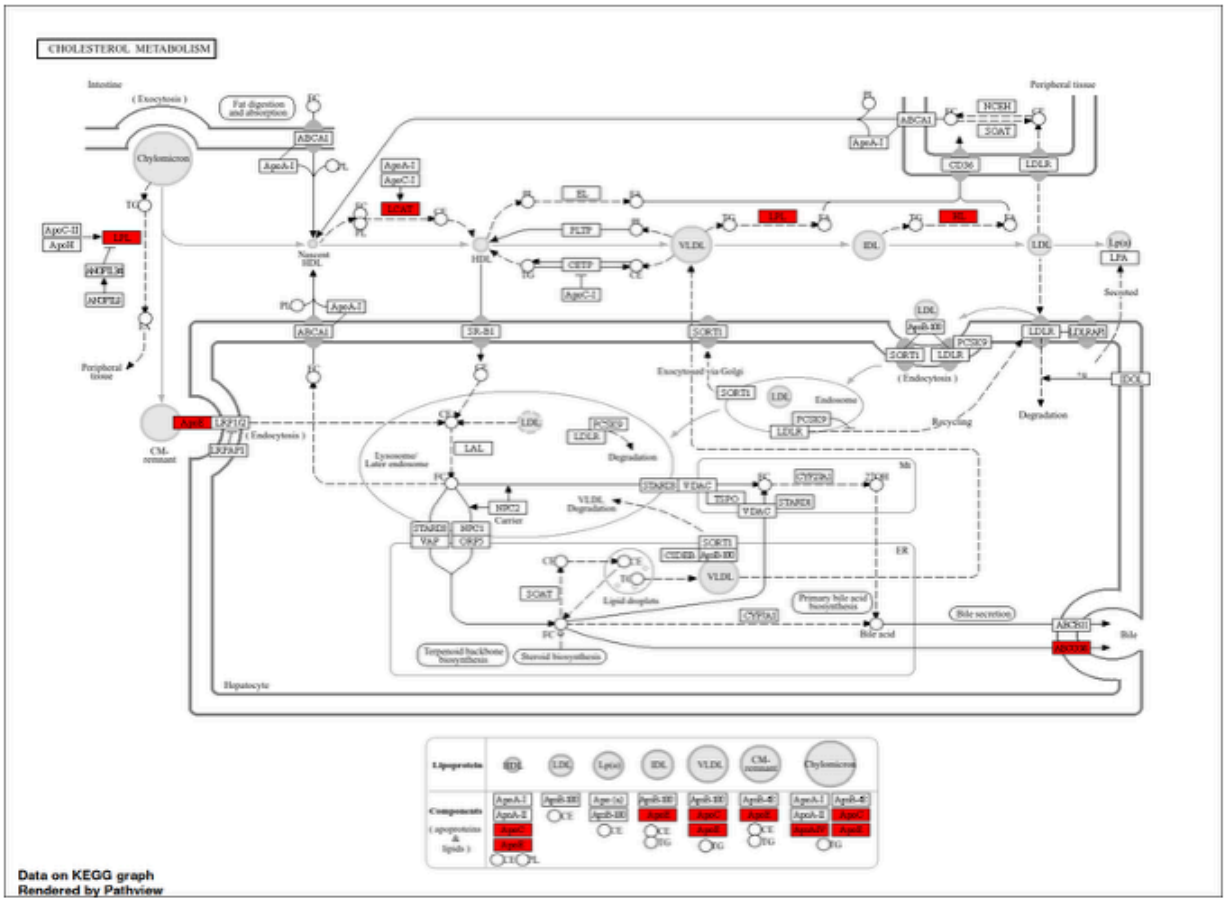


Figure 3

KEGG pathway representing cholesterol metabolism, with critical hub gene involvement highlighted. The pathway illustrates multiple downstream signalling cascades in steroid biosynthesis, terpenoid backbone biosynthesis, and bile secretion.

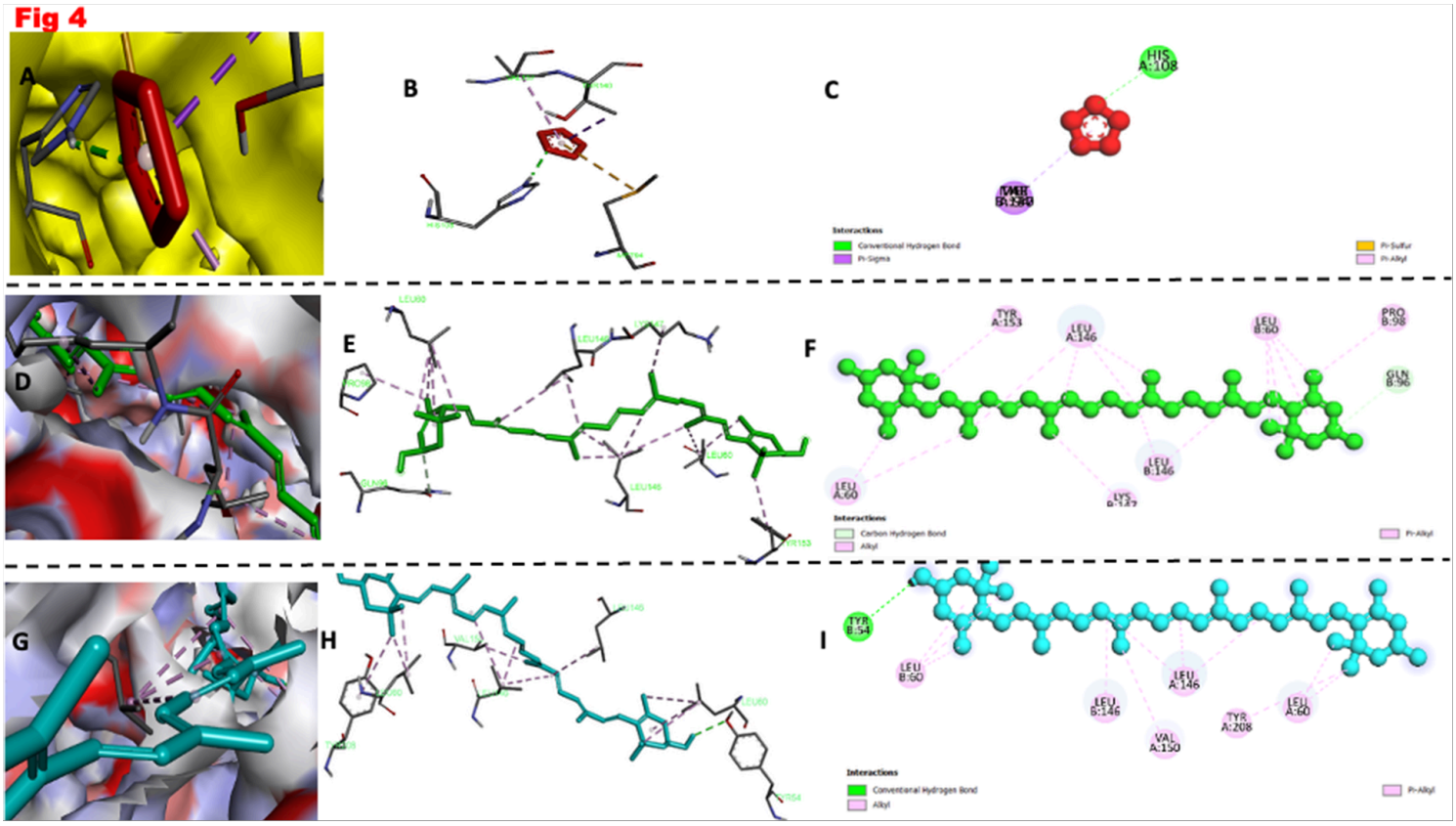


Figure 4

Molecular interaction and docking poses of GST with Furan, LUT and ZEA. **A-C**: Furan moderately interacted with the sidechain amino acid residues at the active site of GST with a docking score: -3.1 kcal/mol. The only appreciable hydrogen bond interaction (2.2 Å) was detected on HIS 108. **Figure 4C** shows that the amino acid residues MET94, THR140 and VAL137 show overlapping positions around the ligand **D-F**: LUT moderately interacts with the sidechain amino acid residues at the active site of GST with a docking score: -5.2 kcal/mol. The only appreciable hydrogen bond interaction (3.1 Å) was detected at GLN 96. **G-I**: ZEA moderately interacts with the sidechain amino acid residues at the active site of GST with a docking score of -3.6 kcal/mol. The only appreciable hydrogen bond interaction (2.9 Å) was detected on TYR 54. GST: glutathione-s-transferase; LUT: Lutein, and ZEA: zeaxanthin.

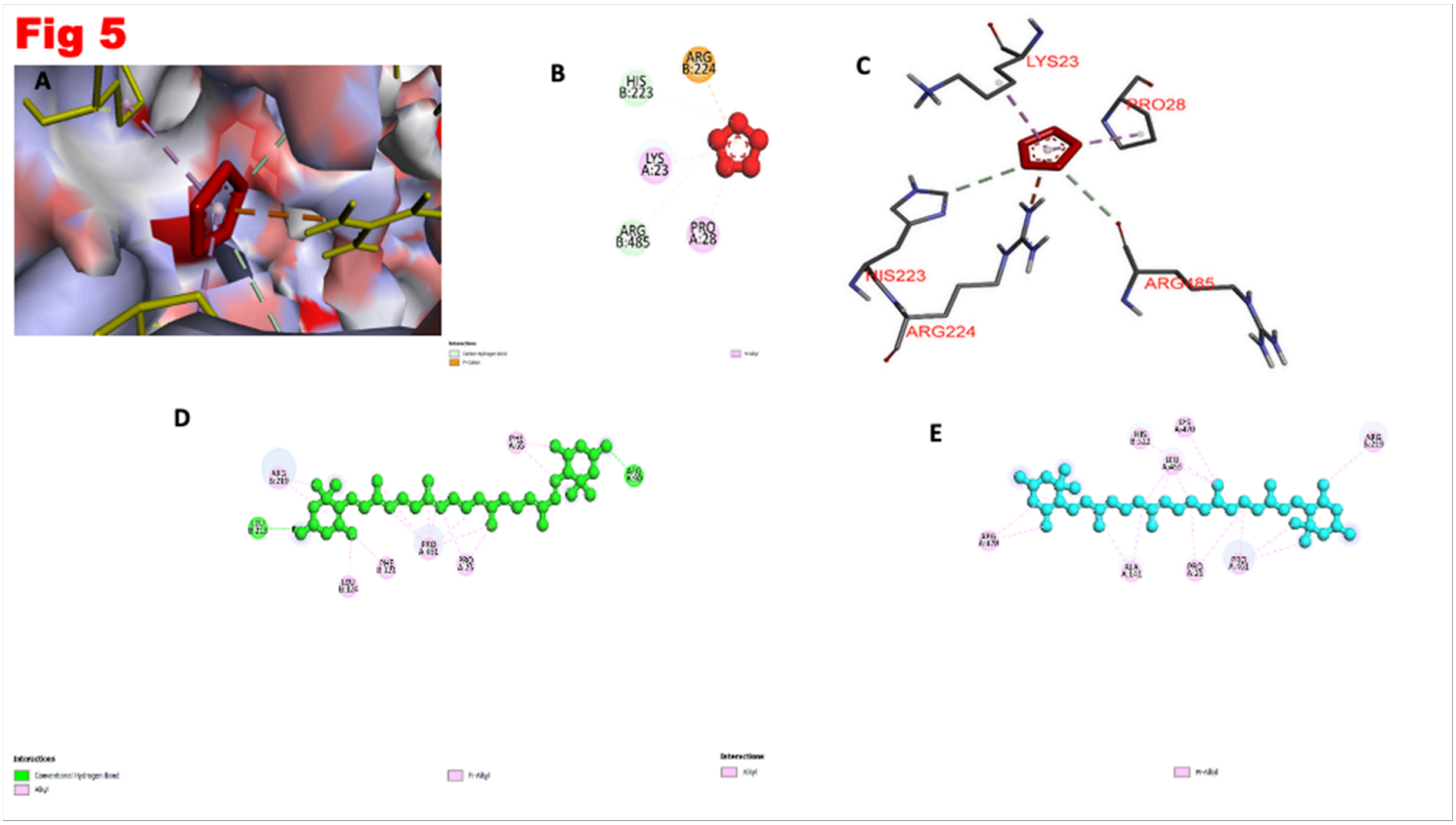


Figure 5

Molecular interaction and docking poses of ACHE with Furan, LUT and ZEA. **A-C:** Furan interacts moderately with the sidechain amino acid residues at the active site of ACHE, docking score: -3.1 kcal/mol. Two hydrogen bonds were detected on HIS 223 (3.6 Å) and ARG 485 (3.6 Å). **D:** Interaction diagram of LUT docked to ACHE showing two hydrogen bonds with LEU 213 (2.0 Å) and ARG 90 (2.0 Å) with docking score: -7.6 kcal/mol. **E:** Interaction diagram of ZEA docked to ACHE, there is no appreciable hydrogen bond with additional π- interaction with surrounding residue, with docking score: -4.9 kcal/mol. ACHE: acetylcholinesterase; ZEA: zeaxanthin, LUT: lutein.

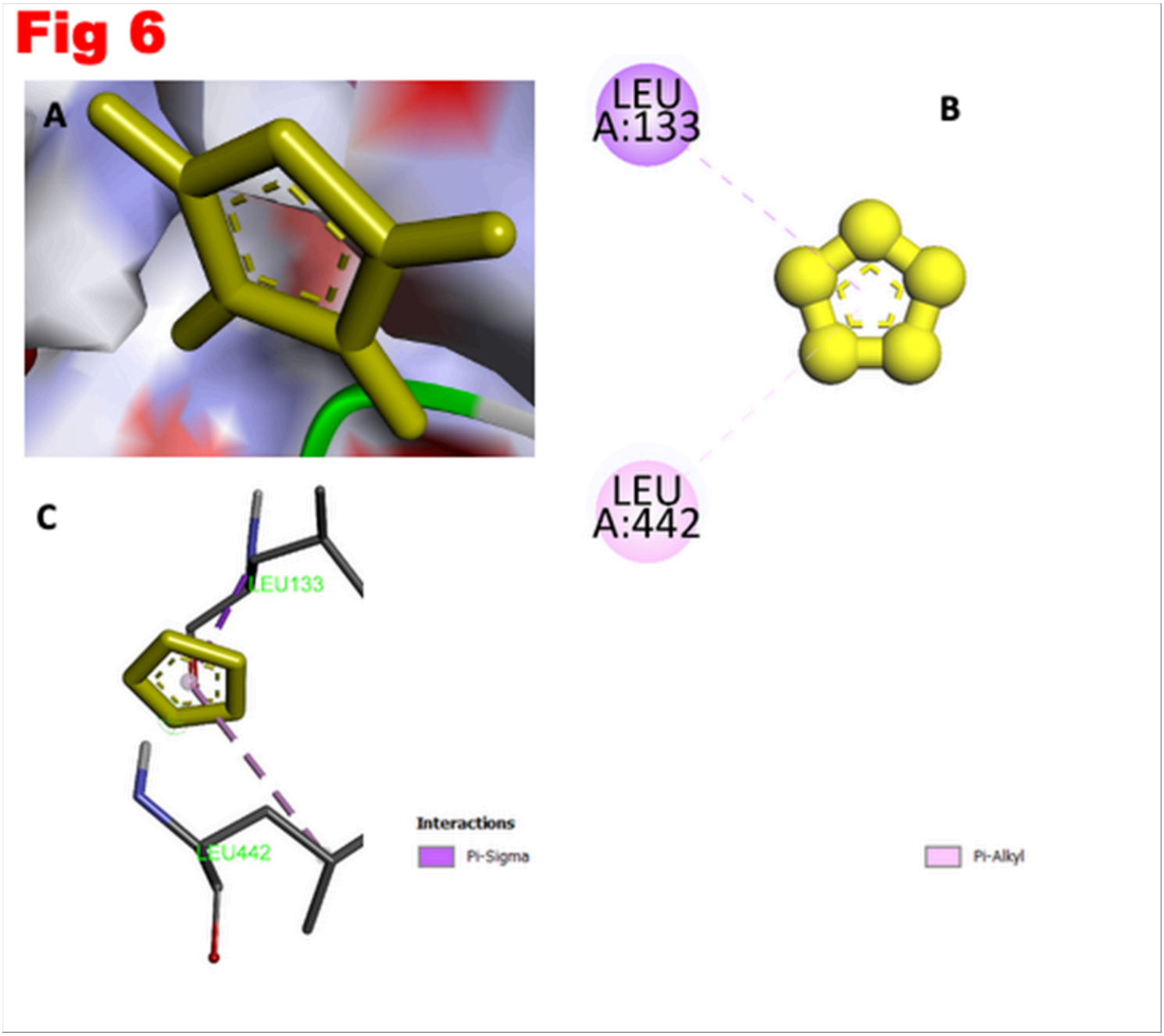


Figure 6

Molecular interaction and docking poses of CYP2E1 with Furan, with a docking score of -2.8kcal/mol. A: surface view of furan in the pocket of the CYP2E1 active site. B: 2D Interaction diagram showing two hydrophobic bonds with LEU 133 (3.62 Å) and LEU 442 (4.70 Å). C: Cartoon view showing the hydrophobic bonds between furan and the two leucine residues.

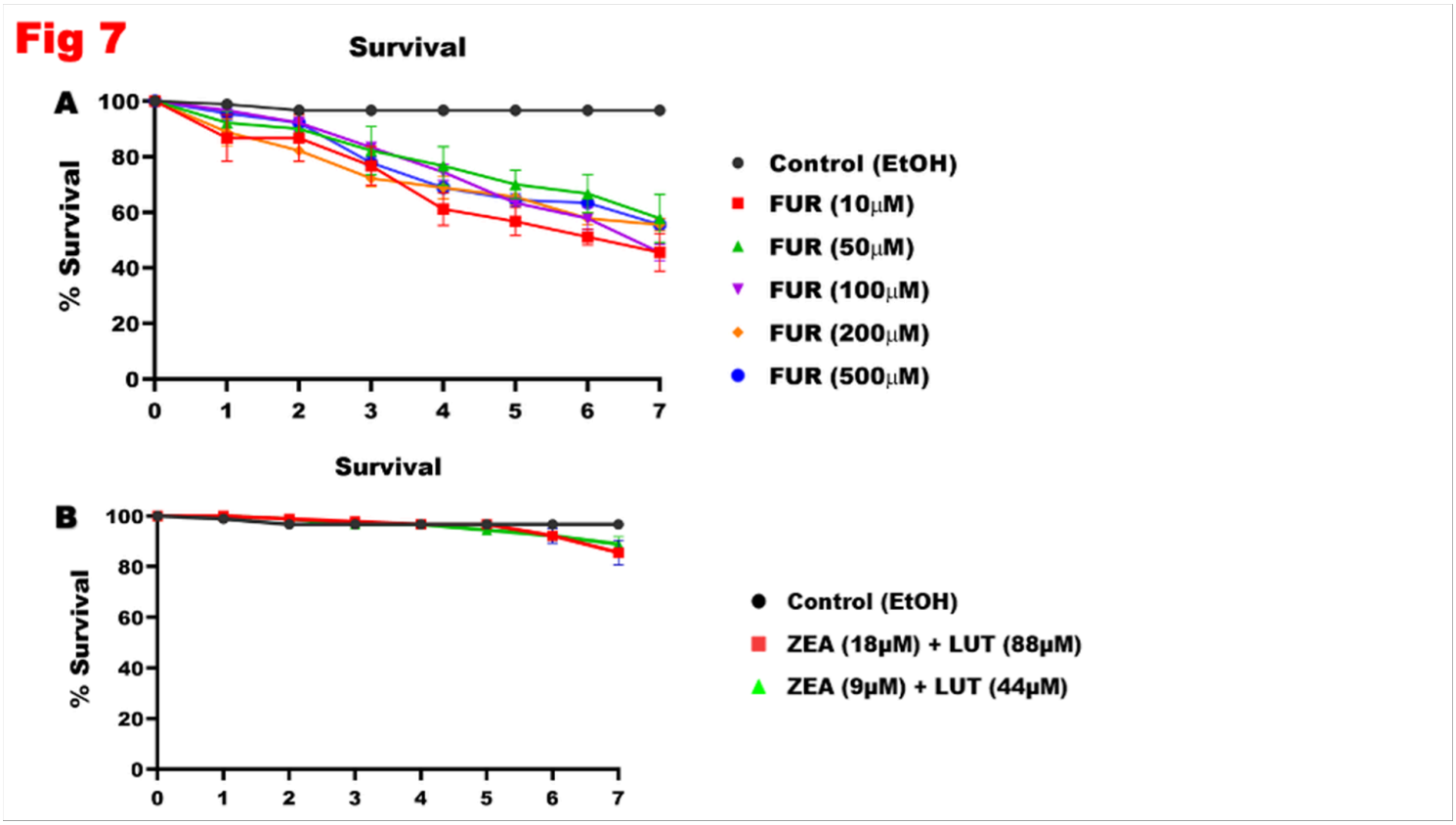


Figure 7

Effect of Furan (A), and Zeaxanthin and Lutein combination (B) on the survival rate *of D. melanogaster.*

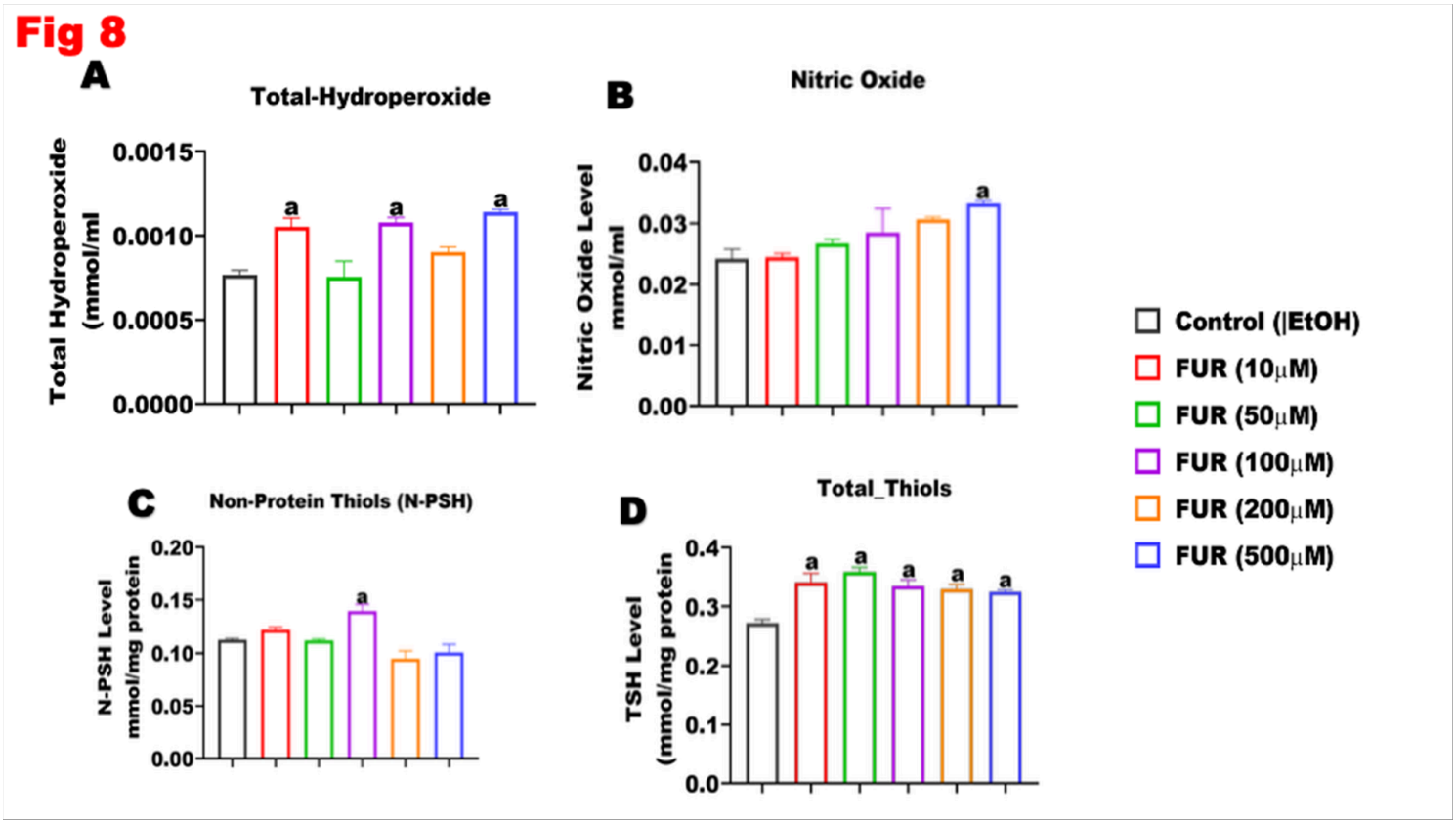


Figure 8

Furan-induced toxicity in Drosophila after seven days of exposure. Total hydroperoxide (A), nitric oxide (B), non-protein thiols (C) and total thiols (D). Data are represented as Mean + SEMof 50 flies per replicate (n = 5) “a” Significantly different from control at *p<0.05*.

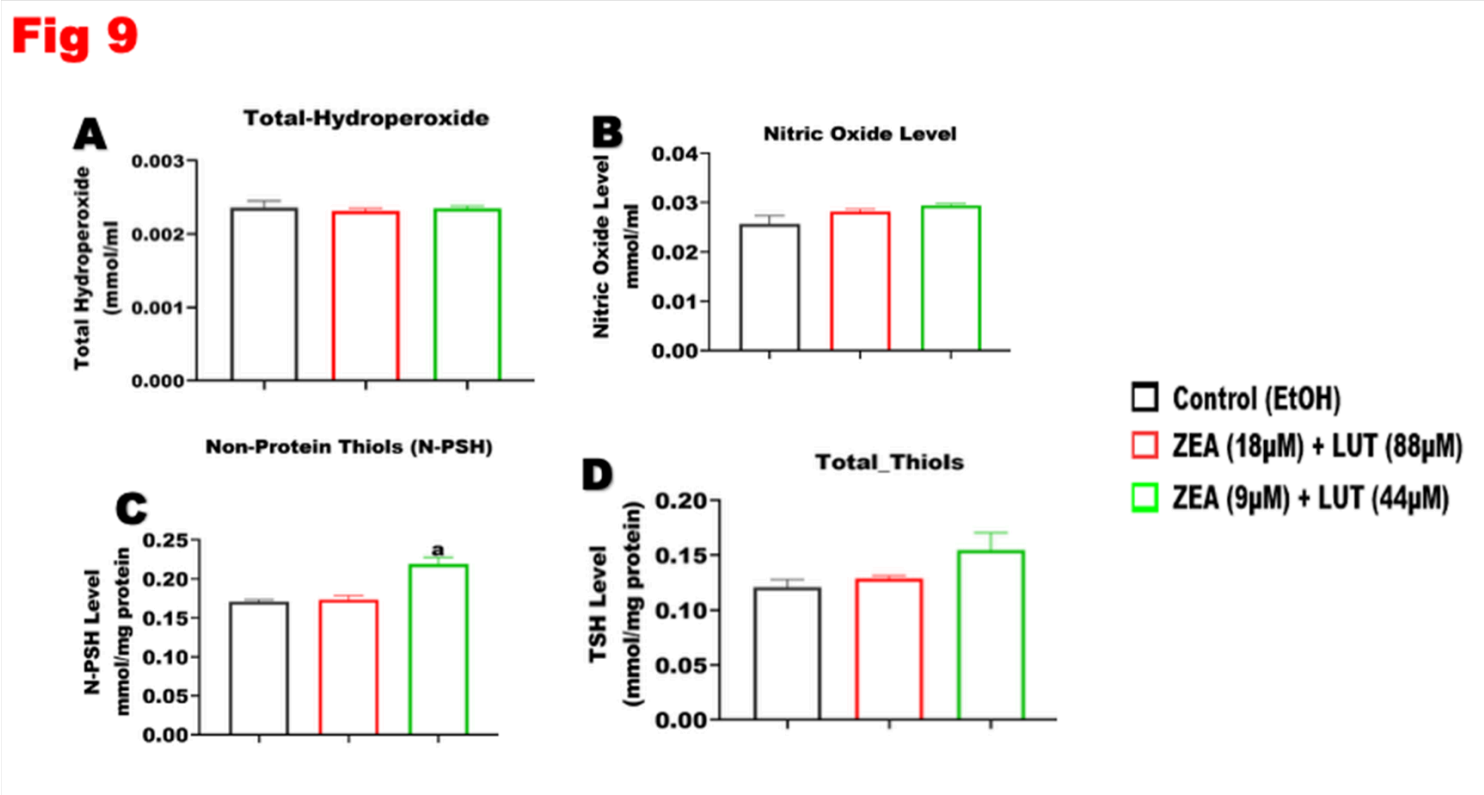


Figure 9

Effect of Zeaxanthin and Lutein combination on Drosophila after seven days of exposure. Total Hydroperoxide (A), Nitric Oxide (B), Non-protein Thiols (C) and Total Thiols (D). Data are represented as Mean + SEM of 50 flies per replicate (n = 5) “a” Significantly different from control at *p<0.05*.

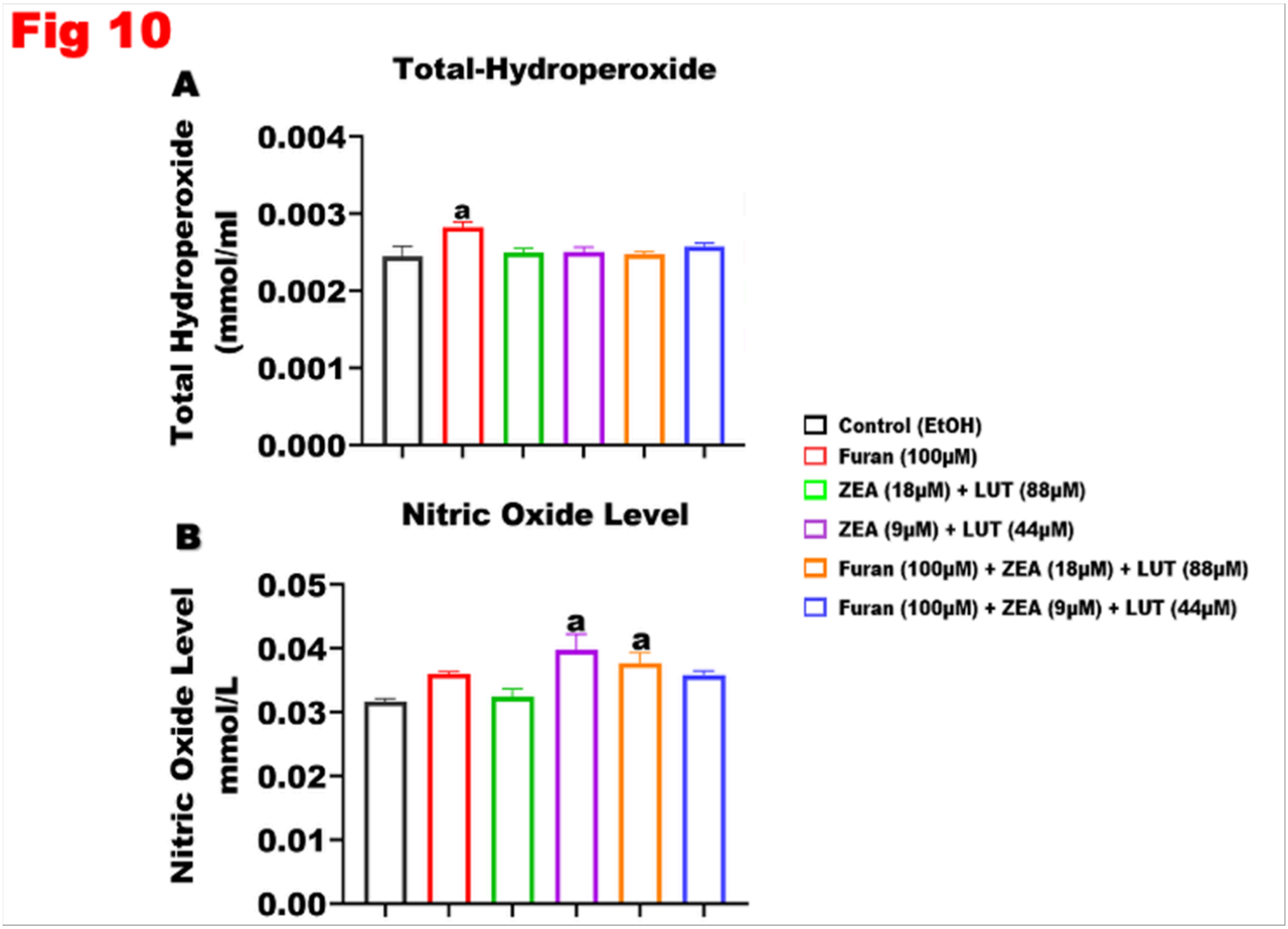


Figure 10

Effect of Zeaxanthin and Lutein combination and/ or Furan on markers of oxidative stress in D. melanogaster (Total Hydroperoxide (A), Nitric Oxide (B)). Data are represented as Mean + SEM, n = 5 “a, and b,” Significant differences with Control and Furan Group at $p<0.05$, respectively.

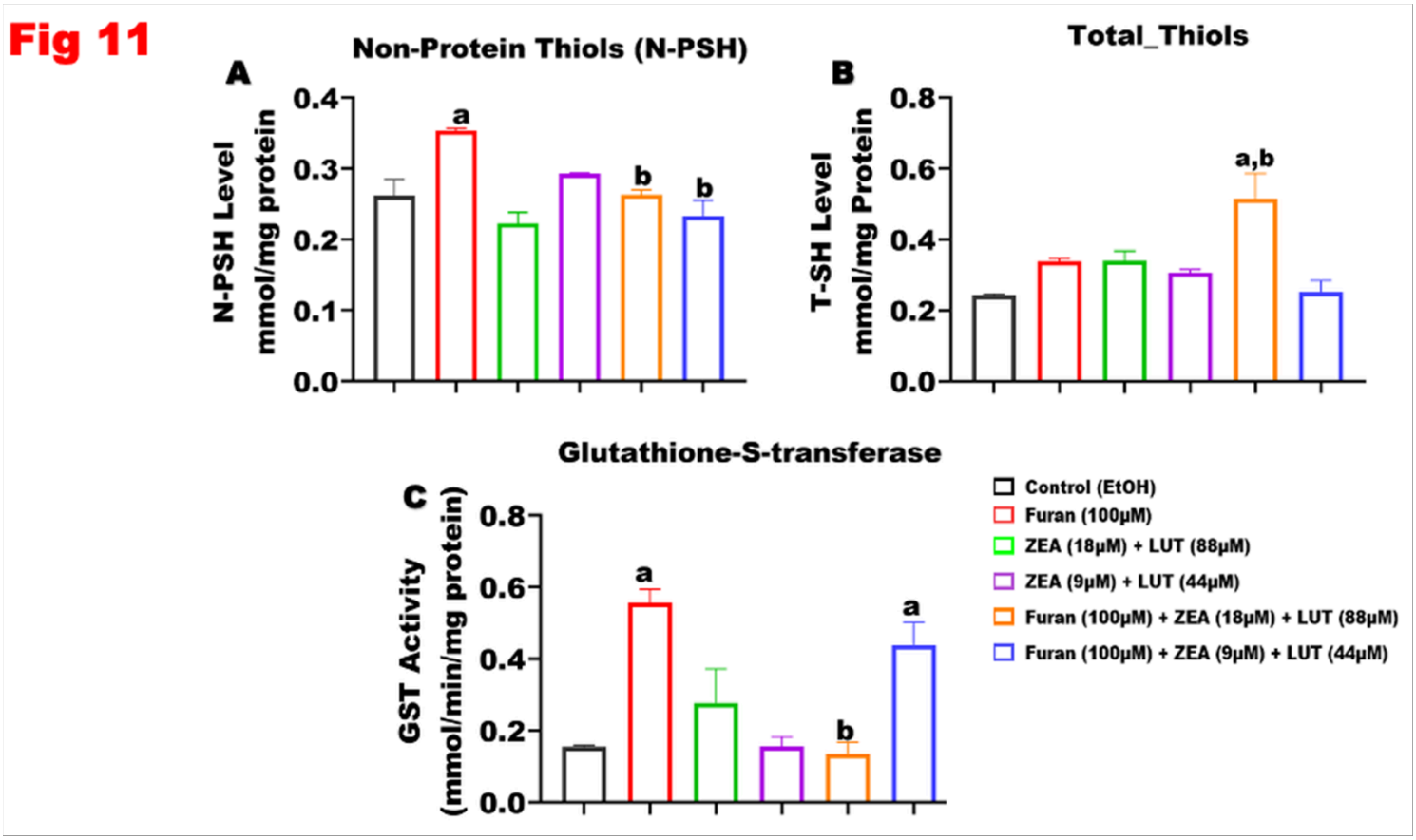


Figure 11

Effect of Zeaxanthin and Lutein combination and/ or Furan Antioxidant markers in *D. melanogaster* (Non-protein Thiols (A), Total Thiols (C) and Glutathione-s-transferase (C)). Data are represented as Mean + SEM, n = 5 “a,and b,” Significantly different from Control and Furan Group at $p < 0.05$, respectively.

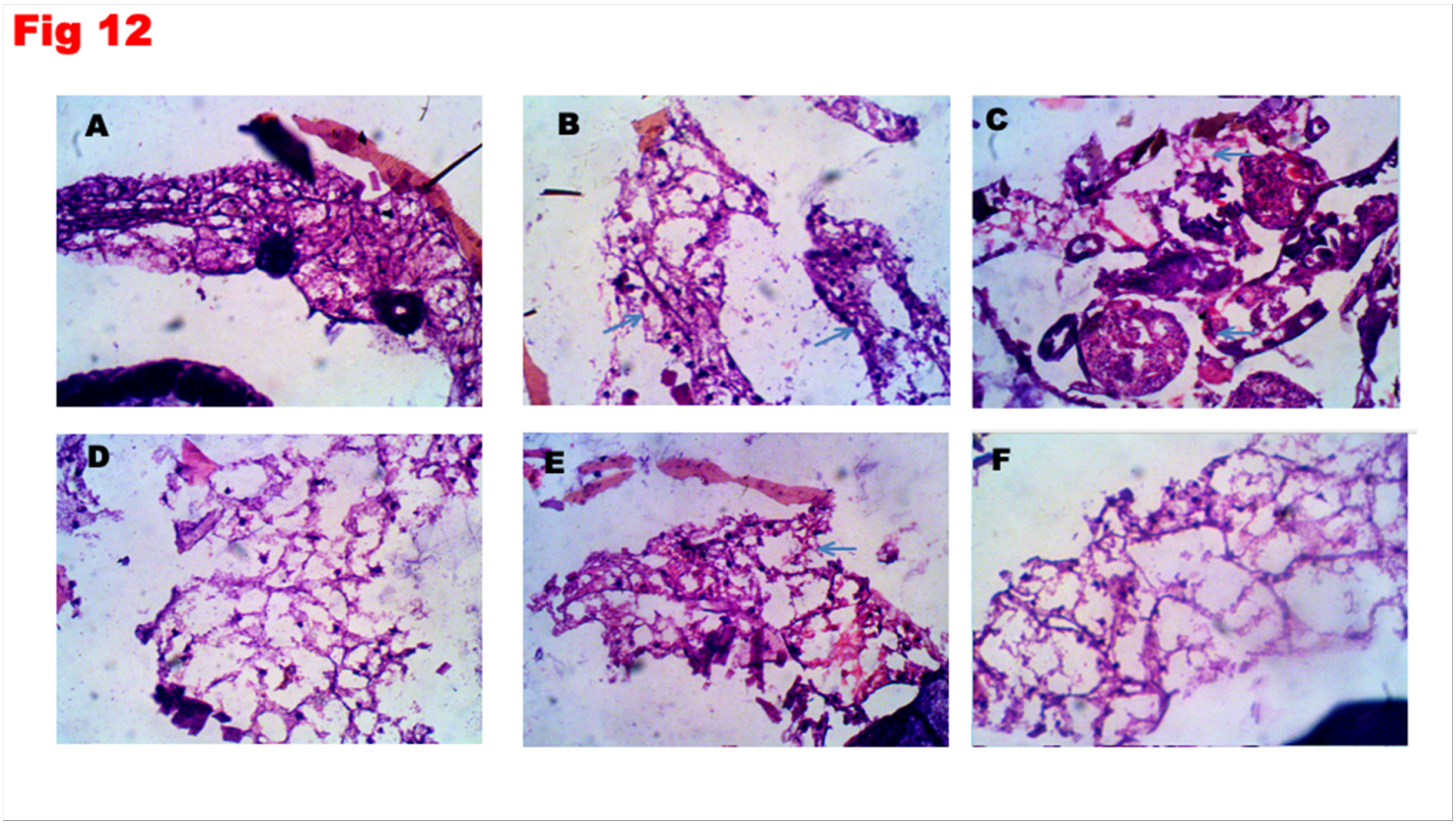


Figure 12

Photomicrographs of the fly's Fat body, Control (A), Furan (B), lutein-zeaxanthin combination at 88μM+18μM (C), at 44μM+9μM (D), co-exposure of Furan and lutein-zeaxanthin combination at 88μM+18μM (E) and 44μM+9μM (F (HE x400)

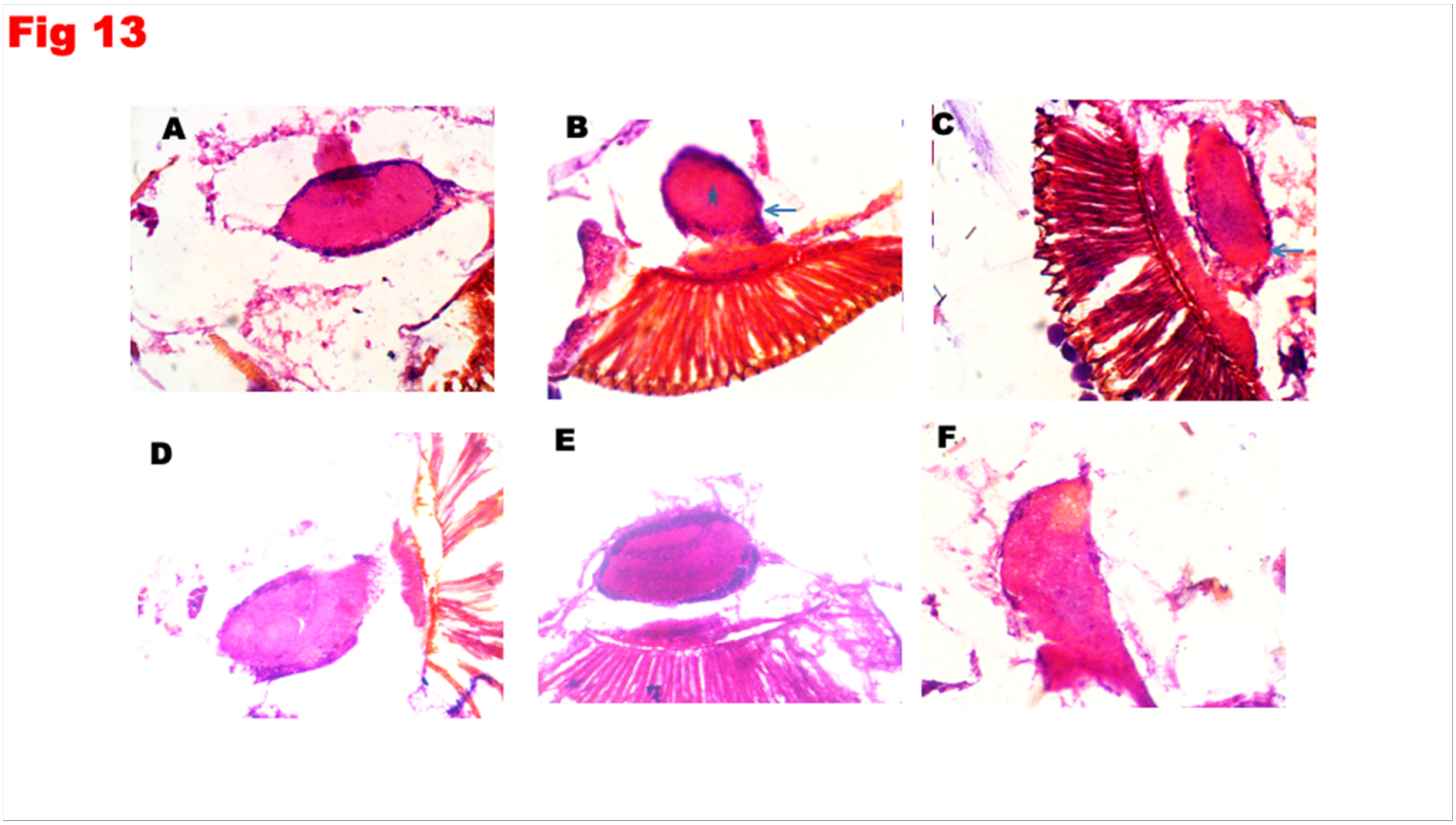


Figure 13

Photomicrographs of the fly Brians, Control (A), Furan (B), lutein-zeaxanthin combination at 88μM+18μM (C), at 44μM+9μM (D), co-exposure of furan and lutein-zeaxanthin combination at 88μM+18μM (E) and at 44μM+9μM (F (HE x400)

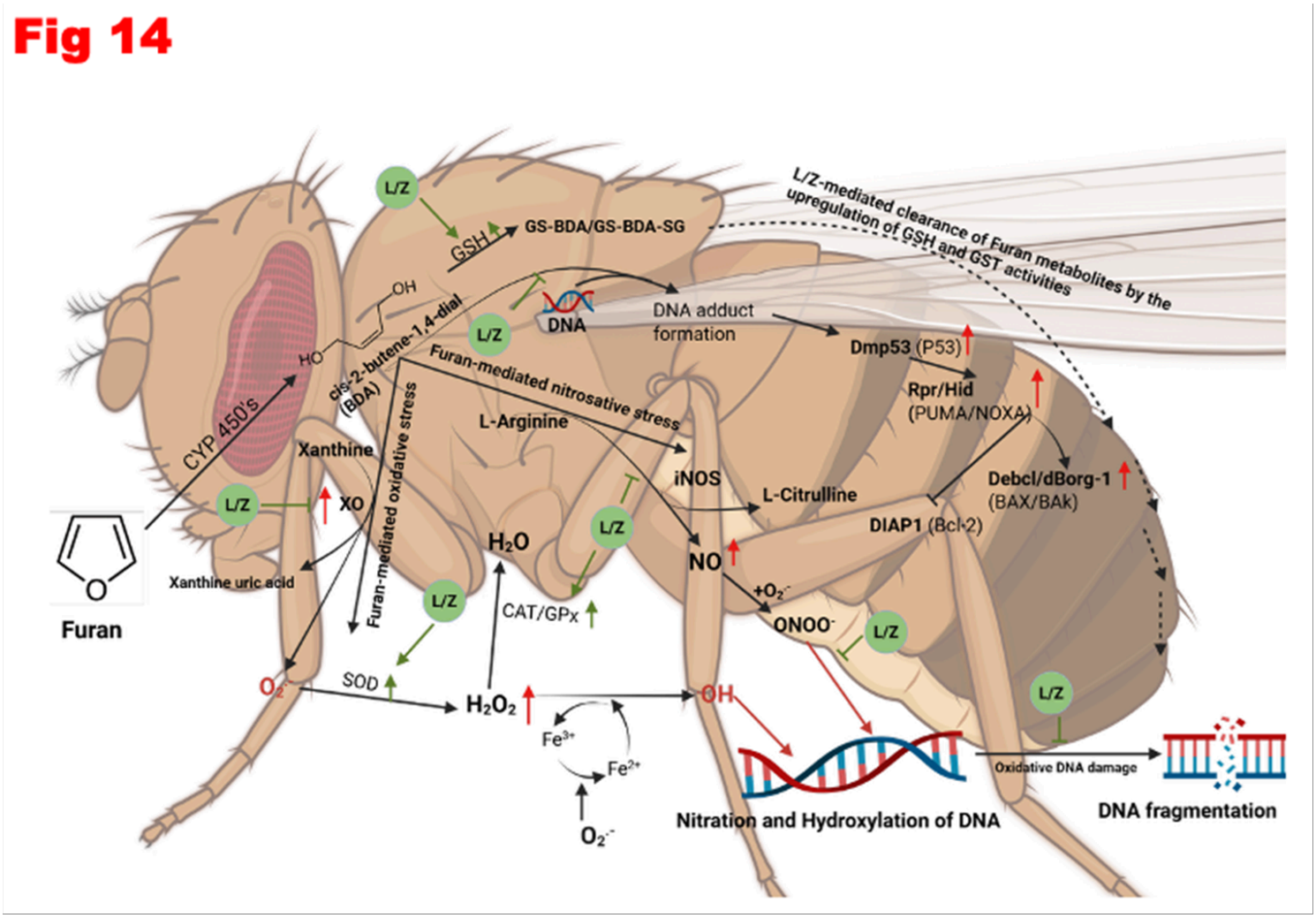


Figure 14

(**A**) Venn diagram showing the intersection between genes targeted by furan and L/Z induced protection (LZP). (**B**) Protein-protein interaction (PPI) network of the 47 common genes between furan and LZP. The network shows interactions among proteins encoded by these genes.

Supplementary Files

This is a list of supplementary files associated with this preprint. Click to download.

- Tablesmanuscript1.docx